LA-UR-13-28967
Approved for public release; distribution is unlimited.

Title: A Technical Demonstration of the Initial Stage of Mo-99 Recovery from a Low Enriched Uranium Sulfate Solution

Author(s): May, Iain
Rios, Daniel
Anderson, Aaron S.
Bitteker, Leo J. Jr.
Copping, Roy
Dale, Gregory E.
Dalmas, Dale A.
Gallegos, Michael J.
Garcia, Eduardo
Kelsey, Charles T. IV
Mocko, Michal
Reilly, Sean D.
Stephens, Francis H.
Taw, Felicia L.
Woloshun, Keith A.

Intended for: Report for NNSA's Global Threat Reduction Initiative program - an open source report is requested
Report

Issued: 2013-11-21

LOS ALAMOS NATIONAL LABORATORY

A Technical Demonstration of the Initial Stage of Mo-99 Recovery from a Low Enriched Uranium Sulfate Solution

The Target 4 'Loop Test' Experiments

D. Rios (C-IIAC), A.S. Anderson (C-PCS), L.J. Bitteker (LANSCE-NS), R. Copping (C-IIAC), G.E. Dale (AOT-HPE), D.A. Dalmas (AOT-HPE), M.J. Gallegos (C-NR), E. Garcia (C-NR), C.T. Kelsey IV (LANSCE-LC), I. May (C-IIAC), M. Mocko (LANSCE-LC), S.D. Reilly (C-IIAC), F.H. Stephens (C-IIAC), F.L. Taw (C-NR) & K.A. Woloshun (AOT-MDE)

9/30/2013

In support of the commercialization of the SHINE Medical Technologies production process we report results that confirming the technical viability of the initial stage of Mo-99 recovery from a Low Enriched Uranium (LEU) sulfate solution, a direct downscale demonstration of the proposed industrial separation process. From a flow sheet designed by Argonne National Laboratory a series of experimental validations was undertaken at Los Alamos National Laboratory. This involved developing methodologies for the preparation/analysis of uranium sulfate fuel, safely containing the fuel during irradiation using a LANSCE capability specifically developed for such irradiations, and chemical flow sheet testing using a titania column. Near quantitative recovery of separated Mo-99 and uranium fuel products were observed post-titania column separation, the uranium recovery allowing for the possibility of fuel recycle. The feasibility of recycle has also been confirmed by re-irradiating the LEU fuel that had passed through the column separation process, and then once again separating out the fission generated Mo-99 in a second column separation process. Thereafter, the feasibility of recycle was further confirmed by re-irradiating the LEU fuel that has passed through the second column separation process, and then once again separating out the fission generated Mo-99 in a third column separation process. This cycle of irradiations and separation chemistry also allowed for the determination of radioisotopes which would contaminate both the LEU sulfate product for recycle, including Ru-103, I-131 & Ce-141, and the Mo-99 product, including Ru-103, I-131 & Te-132. For each of the three LEU sulfate solution sample irradiations, and 'cold-test' sample irradiations with water and dilute sulfuric acid, gas samples were collected. Gas sample analysis revealed both the radiolysis of water in the LEU sulfate samples and provided insight into corrosion of stainless steel by sulfuric acid.

Contents

1. Introduction

Every year 30 million diagnostic procedures are performed worldwide using ^{99m}Tc, a radioisotope with a 6 hour half-life. Over half of these imaging procedures are performed in the United States.[1] ^{99m}Tc is generated from β- decay of ^{99}Mo (2.7 day half-life), which is in turn produced from fission of ^{235}U targets (^{99}Mo fission yield 6.1%) in nuclear reactors around the world.[2] Currently both HEU (high enriched uranium, >20% enriched in ^{235}U) and LEU (low enriched uranium, <20% enriched in ^{235}U) targets are being used to produce ^{99}Mo; with the use of HEU in the process of being phased out in most countries due to proliferation concerns. At presentl Argentina, South Africa and Australia are the only countries solely using LEU solid targets for ^{99}Mo production.[3] The over reliance on aging reactors, one of which is scheduled to cease ^{99}Mo production by 2016 (National Research Universal reactor, Chalk River, Canada), has led to supply shortage and renewed interest in the domestic production of ^{99}Mo using non-HEU technologies.[1,4]

Current chemical processing techniques for the recovery of ^{99}Mo from irradiated solid HEU or LEU targets start with a target dissolution process.[5] Both the aqueous homogenous reactor concept and accelerator-driven technology for ^{99}Mo production would utilize low acidity aqueous LEU target fuels; the later system being developed by SHINE Medical Technologies Inc.[6] There is the potential to recycle LEU solution fuels if the ^{99}Mo can be recovered from the vast excess of irradiated uranium solution,[7] with titania based sorbents being proposed for efficient ^{99}Mo recovery from both uranyl sulfate and uranyl nitrate fuels.[7-9] Previously we have shown that ^{99}Mo can be effectively recovered from both irradiated uranium nitrate and irradiated uranium sulfate solutions using titania sorbent,[10] with the higher radiolytic stability of sulfate *vs*. nitrate making it an attractive media for aqueous solution based LEU production of ^{99}Mo.[7] The next step in process development is to confirm that high % ^{99}Mo recovery can be achieved using a column separation process that more accurately reflects process conditions, a direct downscale of plant operation both in terms of volume of target fuel and, ultimately, ^{99}Mo process activity levels. We now report the use of sample containment for irradiation of up to 150 mL of solution, access to a new capability for multiple irradiations at LANSCE (Los Alamos Neutron Science Center), the development of a semi-automated titania column separation apparatus for separation of ^{99}Mo and separation chemistry results on both first time irradiated and recycled and re-irradiated target solutions. A preliminary report on this work was presented at the April 2013 ^{99}Mo Topical Meeting in Chicago.[11]

2. Experimental

2.1. General Chemical Experimental Details

This work was conducted in specialist facilities using all appropriate chemical and radiological controls, with calibrated pipettes, balances and check weights. All pH measurements were made using an Accumet AR15 pH meter and an Orion ROSS combination pH electrode filled with 3 M aqueous KI. The pH electrode was calibrated using a combination of standard pH 1, 2, 3, 4, 7 & 10 buffer solutions, the exact choice of buffer solutions used depending on the pH range of the samples to be measured. Solution UV/Vis spectra were recorded on a Varian Cary 500 spectrophotometer in standard 1 cm path length quartz spectrometry cells. Raman spectra were collected as solutions in 3 mL glass sample vials on a ThermoFisher DXR SmartRaman with a 12817.33 cm^{-1} Raman laser frequency. Gas-handling operations were undertaken in a fume hood using a manifold built in-house using stock Swagelok/Cajon parts. An MKS pressure transducer and micro-pirani vacuum gauge were attached to the manifold to record pressure readings. The LEU used in this work was provided as a uranyl nitrate aqueous solution from LANL stocks. The % enriched for this stock was reported to be 19.67 atom/atom % (19.54 weight/weight %) ^{235}U. The sample was assayed again for this project by M.C. Filler (LANL) using a Perkin DRC II ICP-MS (Inductively Couple Plasma - Mass Spectrometry), yielding enrichment values of 19.3(±9) atom/atom % and 19.1(±9) weight/weight % ^{235}U *i.e.* in good agreement with the original reported numbers. An experimental flow diagram outlining the main processing steps undertaken is shown in Figure 1.

2.2. Uranyl Molar Absorptivity (ε) Determination for UV-Vis Spectroscopy Uranium Concentration Measurements

Depleted uranium (uranyl(VI)) standard solutions in nitric acid (9.989(±30) g L^{-1} U) were converted to sulfuric acid standard solutions, which were then used to determine the molar absorptivity (ε, in L mol^{-1} cm^{-1}) of the visible spectrum λ_{max} peak of uranium in 1 mol L^{-1} H_2SO_4.[12] This was used as the basis of the development of a simple technique for the assay analysis of the uranium sulfate fuel, and all uranium containing column fractions post-titania separation of the irradiated LEU sulfate fuel (see section 2.3.3.). In order to determine uranyl(VI) concentration by UV/Vis spectroscopy ε must be predetermined. Giving that ε, and λ_{max}, for a particular uranyl species in solution are dependent upon coordination environment it is essential that the anion concentration (in this case HSO_4^-) remains constant when calculating U concentration using Beer-Lambert Law: -

$$A = \varepsilon c l$$

Where A = the absorbance, ε = molar absorptivity (L mol^{-1} cm^{-1}), c = the concentration (mol L^{-1}) and l = the path length of the cell (in this case 1 cm).

ε and λ_{max} of uranyl in 1 mol L^{-1} H_2SO_4 were determined according to the following procedure. In a typical sample preparation an accurately measured aliquot of uranium nitrate standard solution (9.989 g L^{-1} U, 10 ml) was transferred by Eppendorf pipette to a scintillation vial and the mass of uranium solution recorded. The solution was stirred and heated to dryness at 275 ^{o}C until no further nitrous oxides fumes (brown fumes) were visible, with the solid then heated for a further 30 min. The uranium solids were then allowed to cool to room temperature, stirred in H_2O (*c.a*. 3ml) for 5 min then reheated to 275 ^{o}C until dry, again holding at this temperature for a further 30 min. The sample was then allowed to cool and dissolved in 1 mol L^{-1} H_2SO_4 to a volume of 10 ml using a volumetric flask. A range of solutions with different uranium concentrations were prepared this way, and their spectra used to calculate ε for the 420 nm λ_{max} transition (data presented in Tables 1).

On conversion of uranyl nitrate to sulfate a distinct change in intensity and energy of the main absorption peaks were observed as a result of the different ligand (SO_4^{2-} vs. NO_3^-) coordination environment about the uranyl equatorial plane (Figure 2).[13] These spectral differences can also be used as an indication that nitrate has been removed from the LEU sulfate fuel, although Raman spectroscopy is by far the more sensitive and appropriate technique for this task (section 2.3.2.).

2.3. Preparation and Analysis of Low Enriched Uranium (LEU) Sulfate Fuel Solution

2.3.1. Initial Fuel Preparation

Several portions of LEU nitrate stock solution were converted to LEU sulfate fuel and combined into one solution for use in FY13 irradiation activities. In a typical preparation the initial LEU nitrate stock solution (152 mL, pH 1.11, 29.35 g, 0.124 moles U) was heated to a gentle boil in a conical flask covered with a ribbed watch glass and contained in a secondary heavy duty glass beaker. The solution was evaporated to dryness and heated until no brown nitrous oxide fumes were visible emanating from the resultant brown/red residue. This solid was then allowed to cool to room temperature. Distilled water (*ca.* 50 ml) was added to the solid, with stirring, and the sample heated again to a gentle boil until dry and allowed to cool for several hours to produce yellow solids. The yellow solids were presumed to be a mixture of uranium(VI) oxides/hydroxides and any residual nitrate. 4 mol L^{-1} H_2SO_4 (33.34 ml, 0.133 moles) was

added to the yellow solids and the mixture stirred with a gradual increase in temperature until they had all dissolved. The solution was then reduced in volume through boiling, with stirring, until viscous, and heating continued until no nitrous oxides fumes were visible. The viscous liquid was allowed to cool, dissolved in water and the pH lowered by addition of small aliquots of H_2SO_4 until the desired solution pH was reached, 1.0. If the acidity after the dissolution of the yellow solid had been lower than required, the solution could be heated to a viscous oil and then the temperature raised further (>300 °C) to remove excess sulfuric acid from the resultant bright yellow solid. During heating sulfuric acid decomposes (evident by the evolution of white gases) to sulfur trioxide (SO_3) and water,[14] resulting in an increase in solution pH on dissolution of the resultant residues in deionized H_2O. Once all the required uranium sulfate solutions were prepared, and the desired solution pH (1.0) and uranium concentration (*ca.* 150 g L^{-1}) was achieved, they were combined. A 1 mL sample of the resultant solution was taken for Raman spectroscopy (section 2.3.2.) and then returned to the fuel stock solution. 3 X 50 µL aliquots of the fuel were also taken for uranium concentration analysis by UV/Vis spectroscopy (section 2.3.3.) and 5 mL for uranium concentration analysis by Davis-Gray titration (section 2.3.4.). The mass of the solution was also recorded, by weighing known volumes of solution in triplicate, in order to calculate the solution density (1.193(1) g mL^{-1}).

2.3.2. Raman spectroscopy of the Fuel

Raman spectroscopy was used to confirm that < 0.5 mole % nitrate (*vs.* uranium) remained in the LEU sulfate solution. This technique has been described previously,[10] with peak assignments based on literature data.[15] The Raman spectrum of the LEU fuel (uranyl(VI) sulfate in pH 1.0 H_2SO_4) is shown in Figure 3. This spectrum shows Raman bands centered at 856 and 976 cm^{-1} corresponding to the $\nu_1(UO_2^{2+})$ and $\nu_1(SO_4^{2-})$ symmetric stretches, respectively. The Raman band at 1045 cm^{-1} is attributed to the symmetric stretching vibration of uncoordinated HSO_4^-, $\nu_1(HSO_4^-)$. The presence of any NO_3^- would clearly be observed as an apparent increase in intensity of $\nu_1(HSO_4^-)$, the intense $\nu_1(NO_3^-)$ stretching vibration observed at the same energy. This spectrum confirms the complete conversion of the uranyl nitrate stock solution to the uranyl sulfate target fuel solution.

2.3.3. Determination of Uranium Concentration in the Fuel by UV-Vis spectroscopy

The uranium concentration of the LEU target fuel sulfate solution was determined by UV-vis absorption spectroscopy using Beer-Lambert law and the uranyl sulfate molar absorptivity calculated to be 13.65(±2) L mol^{-1} cm^{-1} at λ_{max} = 420 nm (determined in section 2.2.). Triplicate assays of approx. 50 µL sulfate solution (accurately determined) dissolved in approx. 2000 µL (accurately determined) 1 mol L^{-1}

H_2SO_4 were analyzed by absorption spectroscopy, and the results shown in Table 2 (1st pre-irradiation LEU sulfate solution). The absorbance spectrum for the first assay is shown in Figure 4. The average absorbance and molar absorptivity were used to determine the uranium concentration in moles per liter, which was then converted to grams per liter using the 237.41 g mol^{-1} 'atomic' weight for 19.54 % enriched in ^{235}U LEU fuel. The actual concentration of the original uranium solution was then determined by correction for sample dilution. Uranium concentrations were determined similarly for the 2nd and 3rd pre-irradiation LEU sulfate solutions (Table 2), post-irradiation LEU sulfate solutions (Table 3), and separated column fractions containing significant uranium concentrations (Tables 4 – 6). Some column fractions were too dilute for assay, so the solution was first taken to dryness, the resultant residue dissolved with known volumes of 1 mol L^{-1} H_2SO_4, and then assayed.

2.3.4. Determination of Uranium Concentration in the Fuel by Davis-Gray Titration

A sample of the initial LEU sulfate fuel solution was submitted to Chemistry – Analytical and Actinide Chemistry (C-AAC) for uranium concentration analysis by Davis-Gray titration.[16] A uranium concentration of 125.99 mg g^{-1} (±0.1 %) was determined. The uranium concentration of the sample was converted to 150.3 g L^{-1} using the density of the solution (1.193 g mL^{-1}); a value in excellent agreement with the measurement obtained using UV-Vis spectroscopy (150±1 g L^{-1}).

2.4. Target 4 Sample Preparation, Containment, Gas Handling, and Irradiation

2.4.1. Sample Preparation

In total five samples were irradiated; deionized water and 0.1 mol L^{-1} H_2SO_4 samples to 'cold test' the sample containment vessels and three LEU sulfate solution samples. In each case samples were transferred to the inner stainless containers by means of 250 mL wash bottles to minimize loss of material. Details regarding the sample containers are provided in section 2.4.3. The deionized water and 0.1 mol L^{-1} H_2SO_4 Target 4 sample solution volumes (150 mL) were measured using a graduated cylinder. Two gold foil pieces (one inside a plastic bag and the other inside a cadmium envelope wrapped in a separate plastic bag) were taped to the bottom of the inner container holding 150 mL of deionized water. The gold foils were analyzed for activation post-irradiation by gamma spectroscopy which was used to calculate the neutron flux during irradiation.

The three LEU sulfate solutions for the 1st, 2nd, and 3rd irradiations were spiked with small aliquots (53.0, 52.7 and 52.6 µL, respectively) of natural molybdenum from a 10.08 mmol L^{-1} molybdenum stock solution prepared from $Na_2MoO_4.2H_2O$ before being added to the inner containers, to mimic the

molybdenum concentration at proposed SHINE production level sample irradiation (see Table 7). The 2nd irradiation target solution was composed of 78 % recycled LEU sulfate solution from the 1st irradiation post-column separation, the remaining sample made up from fresh solution. Similarly, the 3rd irradiation recycled 77% of the LEU sulfate solution from the 2nd irradiation. The three LEU sulfate solutions were transferred into pre-weighted stainless steel inner containers. After addition of the solutions, the inner containers were weighed again to determine the mass of solution, and via solution density, the volume added. Sample irradiation details are provided in Table 7.

2.4.2. Degassing of Sample Prior to Irradiation

A schematic drawing of the manifold used for degassing the inner stainless steel containers is shown in Figure 5 "degassing". A "freeze-pump-thaw" protocol was used to degas the solution and to replace the air in the headspace with argon to minimize the O_2 background during post-irradiation mass spectrometry measurements.

The use of opaque stainless steel cylinders for sample containment made it impossible to directly observe the freezing/thawing process. To test the degassing operation, and determine the lengths of time needed to freeze and thaw a sample, a 250 mL glass Schlenk flask was used in place of a stainless steel container. Since the heat transfer through stainless steel is more efficient than glass, the time that we determined for freezing (5 min) and thawing (30 min) the solution in the glass flask would be comfortably enough to freeze a comparable sample in a stainless steel container. This procedure was tested using deionized water, 0.1 mol L^{-1} H_2SO_4, and 19.5 g L^{-1} depleted uranium (dU) in 0.1 mol L^{-1} sulfuric acid. The degassing procedure developed using the glass flask was then applied directly to the degassing of samples in the inner stainless steel containers.

After introducing the aqueous sample into the inner stainless steel container, the cylinder was fitted with a 3/8" angle needle valve (Swagelok) and attached to the gas handling manifold using a piece of flexible polyethylene tubing. The sample valve (needle valve) was closed and the sample cylinder was slowly immersed in a liquid nitrogen bath to freeze the sample solution contained within. Care had to be taken to avoid freezing the solution too quickly, as was the case with the water sample, because the solution would splash up into the valve and cause it to fail to seal properly upon subsequent freezing steps. While freezing, and with the sample valve closed, the manifold was evacuated to $<10x10^{-3}$ Torr (valves 1, 2, and 5 open and valves 3, 4, and 6 closed), see Figure 5. After the sample was completely frozen, the sample valve was opened, allowing the headspace gas to be removed. The vacuum gauge was monitored until the pressure decreased below $10x10^{-3}$ Torr, and then the sample valve closed. The sample cylinder was removed from the liquid nitrogen bath and immersed quickly in a warm water bath

to thaw the frozen solution for 30 min. In the glass Shlenk flask tests, copious gas evolution from the solution to the headspace was observed during this stage. After the solution was completely thawed, the freeze-pump-thaw process was repeated twice more. Argon (Ar) was introduced into the evacuated cylinder only after the third freeze-pump-thaw cycle. To this end, the argon line was evacuated back to the tank (opened valves 3 and 4). Next, the manifold was closed to vacuum (valve 2), and pure Ar was introduced (the regulator on the Ar cylinder opened). The sample valve was opened, and the Ar cylinder regulator was adjusted to the desired pressure, usually near ambient (ambient pressure is 587 Torr/11.3 psia at 7000' elevation). The sample valve and the manifold (valve 5) were then closed, the sample side was vented (valve 6 opened), and the sample cylinder/valve assembly was removed from the manifold. The outlet side of the angle valve on the inner container was covered with parafilm to prevent the entry of moderator water after insertion in the outer stainless steel container. It was found that keeping the outlet side of the angle valve dry was important to get a good vacuum seal post-irradiation. The handle of the angle valve was then removed and replaced with the lid of the outer container prior to inserting the inner container into the outer container which contained 500 mL of deionized water, as mentioned above (and see section 2.4.3.).

2.4.3. Sample Containment and Shipment

The solution samples were held within specially fabricated stainless steel inner containers which were sealed with a Swagelok stainless steel needle valve and held inside stainless steel outer containers. The volumes of the inner containers were 210 mL each and the vessels were designed to withstand 150 psi of pressure. The volume of the outer containers were 1000 mL each and they were designed to withstand 25 psi of pressure. The double containment design provided for two layers of containment in case of a loss of inner container integrity. Only high radiation resistance plastic components were used, for both the outer bottle O-ring and the inner bottle valve packing. After solution sample filling (section 2.4.1.) and degassing (section 2.4.2.), the handle of the Swagelok valve of the inner container was removed and replaced with the lid of a stainless steel outer container. The inner containers were then inserted into the outer containers and screwed to hand tight. The sample containers are shown in Figure 6. Prior to insertion of an inner container, the outer container would be filled with 500 mL of deionized water to absorb some fission energy during radiation and to provide neutron moderation. The radionuclide inventory of the main radioisotopes contained in the inner containers was written on yellow tape and stuck on the outside of the outer container. The joint between the base and lid of the outer containers was then sealed with rad tape to make sure sample integrity persisted though sample shipment from TA-48 to LANSCE (Target 4), sample irradiation at LANSCE and subsequent shipment back

to TA-48. The samples were packed and shipped to LANSCE inside a steel Viking container, the authorized container for sample transportation (see picture 1).

2.4.4. Sample Irradiation

The samples were irradiated via a new sample delivery and retrieval capability installed at the LANSCE Target 4 facility, using neutrons produced through bombardment of a tungsten spallation target with a 800 MeV proton beam. Neutrons from the spallation target are thermalized with a graphite annulus surrounding the sample. The thermal neutron flux at the sample location was measured with bare and cadmium covered gold foils to be 1.2 x 10^9 n/(cm^2/S) for an average beam current of 1.3 µA (discussed in section 3.1). Samples (water, H_2SO_4, 1st, 2nd and 3rd LEU sulfate) were irradiated for a total of 5.4, 9.4, 6.0, 7.2 and 6.7 hours, respectively, at an average beam current of 1.3, 1.3, 1.5, 1.2, and 1.3 µA, respectively. The samples were lowered into and raised from the irradiation assembly using a remotely controlled electric motor. Figure 7 shows a drawing of the irradiation insert assembly with the sample in the lowered position. The sample travels in a PVC pipe surrounded with an annular borated polyethylene shield between the service floor and the graphite annulus. There is a vacuum gate valve below the sample in the raised position that allows the upper portion of the assembly to be lifted for sample retrieval without breach of target crypt vacuum.

Stackable borated polythene shielding pieces were cut to fit around the steel cased annular shielding above the insert shown in Figure 7, and assembled to provide a 36-inch tall (36-inch outer diameter) shield around the annular shield. The impact of this additional shielding is incorporated in the MCNPX model geometry plotted in Figure 8. Mesh tally calculated dose rates outside shielding were all less than 5 mrem/h/µA. Neutron and photon flux tallies modified by ICRP 74 flux-to-dose rate conversion factors are also incorporated in Figure 8, the yellow to green transition being at approximately 50 mrem/h/µA. The standard Target 4 insert shielding plug configuration was modeled in the second insert (right insert, Figure 8). It consists of three steel plugs topped with a polyethylene plug. For dose rates on top of Target 4 the standard configuration was about one order of magnitude more effective than the irradiation insert configuration. It was expected that the background effect of shine from the irradiation insert on top of Target 4 would be of no greater significance than that from radiation environments in neighboring flight paths with no overhead shielding.

2.4.5. Removal of Headspace Gas from Irradiated Solutions

The procedure for removal of headspace gas for all Irradiated Target 4 samples was the same.

The inner container holding the irradiated solution was attached directly to the gas-handling manifold, as shown in the "Gas Transfer" drawing of Figure 5. The 500 cc gas cylinder (Swagelok), fitted with a bellows valve, was attached to the gas-handling manifold and evacuated to $<10x10^{-3}$ Torr (with valves 1, 2, 4, and 5 open; valves 3, 6 and sample container closed). The manifold and the 500 cc cylinder were then closed to vacuum (valve 2 and gas cylinder valve closed). The sample container valve was then opened and the pressure allowed to expand into the evacuated manifold (15 cc), 500 cc cylinder and 60 cc headspace of the sample container and the pressure recorded. Boyle's Law ($P_1V_1 = P_2V_2$; where P_1 = pressure of gas generated, V_1 = 60 cc headspace of inner container, P_2 = pressure of gas recorded after gas generated expansion, V_2 = combined volumes of 500 cc cylinder + 60 cc headspace + 15 cc manifold volume) was then applied to determine the gas pressure generated during irradiation. Both sample container and gas collection cylinder (500 cc cylinder) valves were then closed and the manifold evacuated (valve 2 opened). The sample side of the manifold was closed to vacuum (valve 5 closed), vented to atmosphere (valve 6 opened), and the solution container and the gas sample cylinder were removed from the manifold. 87 % of the headspace gas would therefore be trapped in the 500 cc stainless steel cylinders. The gas sample cylinder valve opening was fitted with a plug, and the cylinder was stored in the fume hood for a period of at least 2 months to allow radioactive fission product gases to decay. The sample container was then transferred back to the solution chemistry hood for chemical analysis and separation chemistry of the irradiated solution.

2.5. Irradiated Solution Analysis and Separation Chemistry

2.5.1. Irradiated Solution Analysis

Post-irradiation the 0.1 mol L^{-1} H_2SO_4 sample had a bluish color, indicative of corrosion, and was thus analyzed by both UV-vis spectroscopy and ICP-MS to determine the extent of leaching of transition metals into the solution. ICP-MS analysis was performed by W.S. Kinman (Chemistry – Nuclear and Radiochemistry, LANL). For the three irradiated LEU sulfate solutions the pH values were recorded, the uranium concentrations determined (section 2.3.3.) and the solution densities calculated by weighing known volumes of solution in triplicate (Table 7).

Production activities for all three irradiated LEU sulfate solution were measured by gamma spectroscopy at the TA48 count room, both on 5.0 and 1.25 mL samples of neat irradiated LEU sulfate solutions (accurately measured using calibrated pipettes). The 1.25 mL samples were diluted with 3.75 mL of 0.1 mol L^{-1} H_2SO_4. Samples were analyzed at different times; radioisotopes with shorter half-lives usually yield better count data when the measurement was undertaken close to EOB (End of beam).

Conversely, longer lived radioisotopes often yielded better count data when most of the short lived radioisotopes had decayed. In some cases production activities were calculated after complete ingrowth from parent isotopes, *e.g.* the production activity of ^{131}I was calculated 72 hours after EOB to ensure complete ingrowth of ^{131}I from $^{131m/131}$Te.

2.5.2. Batch Separation Experiments

Batch separation experiments were undertaken in triplicate (samples 1 – 3) for the first irradiated LEU sulfate solution. Titania sorbent (15.4, 14.6 and 14.8 mg; Sachtopore NP 110 µm particle size, 60 Å pore size) was transferred into three 4 mL glass vials and labeled sample 1 – 3, respectively. To each vial 0.992 mL of 0.1 mol L^{-1} H_2SO_4 were added and the vial then left on the bench top undisturbed for 24 hours. This step conditioned the titania sorbent to pH 1, the same pH as the irradiated uranium solution. The conditioned titania sorbents and associated acids were then transferred into 3 separate 10 mL PPCO Oak Ridge tubes and centrifuged at 7000 rpm for 6 min. The H_2SO_4 supernatants were then drawn off the tubes using disposable pipets. 1.49 mL of irradiated LEU sulfate solution was then added to each of the 10 mL PPCO Oak Ridge tubes, which were subsequently transferred into a Thermo Scientific precision digital circulator water bath for shaking (100 rpm) at 70 °C. The experiment was performed at 70 °C instead of, 80 °C the required temperature for direct comparison with the column experiments. This was due to the higher volatility of water at 80 °C, which would have resulted in too much evaporation of the water bath water overnight. The experiment was stopped 22.5 h. later, the Oak Ridge tubes withdrawn from the shaker bath, and then centrifuged at 5000 rpm for 5 min. The yellow supernatant in each tube was drawn off with disposable pipets and each was individually filtered through 3 mL plastic syringes with 0.2 µm PTFE filters, with the supernatants collected into 4 mL glass vials. Sample of filtered irradiated post-contact solutions (1.24 mL) were combined with 3.75 mL of 0.1 mol L^{-1} H_2SO_4 and submitted for gamma spectrometry analysis. The titania sorbets were then washed (twice) by adding 2 x 2.0 ml of deionized water (swirling to mix), followed by centrifugation at 5000 rpm for 5 min, and removal of the water using pipettes. Washing the titania sorbent with water ensured that all the residual irradiated uranium solution was drawn off the sorbent. 1.24 mL of freshly opened 0.1 mol L^{-1} NaOH solution was then added to each tube which were then transferred back into the shaker bath for shaking (100 rpm) at 70 °C. The experiment was again ended 22.5 hours later and the tubes withdrawn. The supernatants from tubes 1 and 2 were drawn off into 3 mL plastic syringes with 0.2 µm PTFE filters and the solutions filtered into 4 mL glass vials, the same procedure was also employed for

the 3rd sample after centrifugation at 5000 rpm for 5 min. A pH value of 12.9 was observed for each sample. 1.24 mL of the basic solution from each vial was transferred into 20 mL scintillation vials containing 3.75 mL of 0.1 mol L^{-1} NaOH solution and the samples submitted for gamma spectrometry analysis. The titania sorbent in tube 3 was washed (twice) by adding 2 x 2.0 ml of deionized water (swirling to mix), followed by centrifugation at 5000 rpm for 5 min, and removing the water using a plastic pipette. The titania sorbent was then combined with 5 mL of deionized water in a 20 mL scintillation vial and submitted for gamma spectroscopy analysis.

2.5.3. Column Separation Process

Separation of ^{99}Mo from uranium and a fraction of the fission products was achieved using semi-automated separation apparatus which was composed of the following general components: source and collection vessels, tubing, column, pumps, valves, heating tapes and a heating block (see Picture 2 and Figure 9). The feed solutions, strip solution and post-column fractions were held in plastic bottles, typically Nalgene or Falcon tubes. From the feed and strip source vessels, 1/8" OD PTFE tubing led to the piston pumps (Eldex A-60-S), and 1/16" OD stainless steel (316) tubing led from the piston pumps to the column via valve heads. Valco multiposition microelectric valves were used at the top and bottom of the column; valves were actuated only when the direction of solution flow was changed. The YMC America column was packed with the same Sachtopore TiO_2 sorbent (NP 110 µm particle size 60 Å pore size) used for the batch experiments (section 2.5.2.). The mass of titania sorbent used in the 1st, 2nd, and 3rd columns were 1.966, 1.917 and 1.833 g, respectively. The column was connected to the stainless steel tubing using Swagelok quick connects.

The input parameters for the column separation experiments were provided by Argonne National Lab. These input parameters were designed to be a direct down-scale of SHINE's planned plant scale column operation and were obtained after running a VERSE (VErsatile Reaction Separation), computational simulation based on ^{99}Mo batch and column separation data, a simulation program developed at the University of Purdue.[9c] Throughout the separation process, the column (which was enclosed inside an aluminum block) and the stainless steel tubing connecting the piston pump and column were heated with heating tape to 80±1 °C. The temperature was set and monitored by a temperature controller. Maintaining this temperature was important for both optimizing ^{99}Mo binding to the column, and even more important for minimizing the volume of base required to strip the entire ^{99}Mo product. The column was pre-equilibrated to pH 1 with a 0.1 mol L^{-1} H_2SO_4 wash before being loaded with the irradiated uranium solution to bind the ^{99}Mo (as $HMoO_4^-$) to the column, then washed with 1 mol L^{-1} H_2SO_4 and finally water – all in an upward flow direction. The acid and water washes were designed to

both ensure all of the irradiated uranium solution was removed from the column and to assist in the removal of other fission product/actinide impurities. After these washing steps it was envisioned that the ^{99}Mo would remain bound to TiO_2 and could be subsequently stripped off the column with 0.1 mol L^{-1} NaOH, added in the downward direction. The original strip solution was planned to be 1 mol L^{-1} NH_4OH but at 80 °C there was concern that ammonia volatilization would cause a pressure build up in the system. The effective decrease in base concentration changing from 1 mol L^{-1} NH_4OH to 0.1 mol L^{-1} NaOH (if not pH) by an order of magnitude resulted in > 15 mL of base being required to completely neutralize the acidity in the column before the ^{99}Mo product could be stripped in a basic solution (see section 3.3.4.). The details of the column design are collated in Table 8.

2.5.4. Iodine Speciation of Irradiated LEU Sulfate Solutions

This method was adapted from the procedure provided by D.C. Stepinski from Argonne National Lab, a procedure in turn adapted from the literature.[17] This procedure was used to separate the most likely iodine species (I_2, I^- and IO_3^-) present in irradiated LEU sulfate solutions, and selected column fractions. Elemental iodine, I_2, was extracted by contacting the sample for analysis (2.0 mL) three times, sequentially, with 2.0 mL of chloroform each time. Nonpolar iodine should readily extract into $CHCl_3$. The three chloroform fractions were then combined and contacted three times, sequentially, with 1.67 mL of 0.1 mol L^{-1} $Na_2S_2O_3$ in 0.1 mol L^{-1} NaOH each time. The aim was to reduce extractable iodine dissolved in chloroform to non-extractable iodide which would strip back into the aqueous phase. The resulting aqueous fractions were combined and submitted for gamma spectroscopy analysis to determine the quantity of I_2 that was present in the original 2.0 mL sample. Iodide, I^-, was extracted by contacting the irradiated solution with 3 x 2.0 mL of chloroform containing 0.01 mol L^{-1} of stable I_2. The radioactive iodide was presumed to undergo rapid isotopic exchange with the vast excess of stable I_2 found in the chloroform, with the aim of obtaining effective quantitative extraction of radio-iodide into the chloroform phase. The three resultant chloroform fractions were then combined and contacted with 3 x 1.67 mL of 0.1 mol L^{-1} $Na_2S_2O_3$ in 0.1 mol L^{-1} NaOH each time to reduce the iodine to aqueous soluble iodide. The resulting aqueous fractions were combined and submitted for gamma spectroscopy analysis to determine the amount of I^- in the original sample. The 2.0 mL of the original sample post chloroform contact was transferred to a 20 mL scintillation vial containing 3.0 mL of 0.1 mol L^{-1} H_2SO_4 and the sample submitted for analysis to determine the amount of un-extractable iodine, presumed to be mainly iodate, IO_3^-. Components of this procedure were first tested with iodine and depleted uranium prior to the experiments with irradiated LEU solution.

2.6. Gas Phase Analysis

The gas fractions collected from the primary stainless steel containers (section 2.4.5.) were analyzed for O_2 and H_2 content > 15 weeks after end of beam (EOB), allowing for volatile radioisotope decay (Figure 5, "Mass Spec"). The mass spectrometer (residual gas analyzer, RGA) used for H_2 and O_2 analysis was a Stanford Research Systems (SRS) RGA-100 head, evacuated by a Varian V-70 turbo pump and backed by an Agilent SH-110 scroll pump. The gas-handling manifold was also fitted with, and evacuated by, a Varian V-70 turbo pump at valve 1 (backed by the same scroll pump) for this step. SRS RGA software was used for data acquisition and analysis. A variable rate leak valve (Brooks/Granville-Phillips) controlled the inlet of gases from the manifold to the RGA. Sensitivity tuning, filament and gauge degassing, and calibration were performed according to the manufacturer's instructions.

The gas-handling manifold was configured as in Figure 5, "Mass Spec". The leak valve (LV) was set to its closed position. A gas mixture—either a calibration gas (4% H_2/Ar and 6% O_2/Ar), or a sample—was attached to the manifold, and the manifold was evacuated to $<1x10^{-5}$ Torr (the limit of the micro-pirani gauge; valves 1, 2, 3, 4, and 5 open and valve 6 closed). After evacuation, the manifold was closed to vacuum (valve 2 closed). Gas samples were added to the manifold, and introduced into the RGA through the LV at a set pressure ($1x10^{-5}$ Torr, as set by the LV and read using an ion gauge at the RGA inlet). The responses to these gases were recorded, and data was saved as a RGA file screen shot and as ASCII data. All relevant valves were then closed (sample valve, valve 5, and the LV), the gas samples were removed (opened, then closed, valve 6), and the manifold was evacuated.

3. Results and Discussion

3.1. Irradiated Water Sample

A deionized water sample (150 mL) was irradiated to 'cold test' sample containment and to provide data on the observed experimental neutron flux. Gold foils (encapsulated and not encapsulated in Cd) taped to the bottom of the inner container were used to determine the fast, total, and thermal neutron fluxes during radiation. The activated gold foils were submitted for gamma spectroscopy analysis and the results are shown in Table 9. Neutron capture of 100 % natural abundance ^{197}Au results in the formation of ^{198}Au with a half-life of 2.69 days, and this activation is used a standard method of determining neutron flux through the ^{198}Au 412 keV gamma transition.[18] The bare foil is used to measure the total neutron flux. The cadmium cover surrounding the encapsulated gold foil absorbs all thermal neutrons, and so the Cd covered gold foil measures only the fast thermal neutron flux. The thermal flux is

determined by subtracting the fast flux from the total flux. A thermal neutron flux of 1.2 x 10^9 m/(cm^2/sec) was calculated using the data obtained from neutron activation of gold at an average beam current of 1.3 μA.

The gas pressure in the inner sample container after irradiation was lower for this sample post-irradiation *vs.* pre-irradiation which could indicate a loss of containment, although it appeared that the primary container had a good seal (see Table 10). The most likely reason for any loss of containment was due to water splashing into the needle valve, which could have prevented a complete seal of the needle valve during the freeze-pump-thaw cycle. However, the observed loss of pressure (-8.6 Torr) is small enough to also be attributed to temperature differences between the pre- and post-irradiation measurements. Certainly for future irradiations it would be advisable to record the temperature every time a gas pressure measurement was being made.

The water contained inside the inner stainless steel container remained colorless after radiation and the β/γ-meter showed no dose upon close contact of the water with the instrument, indicating that no activated metal ions leached into the solution from the stainless steel container. The absence of activated products leaking into the irradiated water sample was confirmed by taking a 5.0 mL sample from the inner container water and submitting for gamma spectroscopy analysis. No above background radioisotope gamma ray energies were observed for this sample.

3.2. Irradiated H_2SO_4 Sample and a Discussion of Acid Corrosion of the Inner Stainless Steel Container

A 0.1 mol L^{-1} sample of H_2SO_4 (150 mL) was irradiated to determine if acid corrosion of the stainless steel could be a concern during irradiation of LEU sulfate solutions. The amount of gas generated by the irradiated sample, 452 torr (Table 10), was calculated as described in section 2.4.5. Analysis of this gas by mass spectrometry determined that hydrogen was the sole gas generated from this solution (Table 11). It is interesting to note that this sample produced greater pressure and more hydrogen gas (Tables 10 and 11) than the LEU sulfate containing samples, which would appear to be the result of the increased corrosive action of dilute H_2SO_4 on the stainless steel 304 vessel in the absence of uranium. Indeed, the solution had a distinct blue coloration when it was decanted from the inner stainless steel container, which indicated the presence of transition metals in the post-irradiation solution. The inner container was fabricated using stainless steel 304 which was made from a mixture of chromium (18 – 20 %), nickel (8 – 11 %), manganese (< 2 %), carbon (< 0.08 %), silicon (< 0.75 %), phosphorous (< 0.045 %), sulfur (< 0.03 %) and iron (the balance). ICP-MS analysis, performed by W. Kinman at C-AAC,

on eight duplicate 100 µL samples of this blue solution confirmed that chromium, nickel, manganese and iron were present, with iron being the most abundant ion in solution (Table 12). The concentrations of the other three transitions metal cations correlated with their % abundance in steel 304. According to ICP-MS the chromium, nickel, manganese and iron concentrations in the 150 mL H_2SO_4 sample post-irradiation were 325, 143, 25 and 1288 ppm (mg L^{-1}), respectively. Only trace amounts of other contaminant (zirconium, niobium, molybdenum, tin, tantalum, tungsten, vanadium, cobalt and copper) at concentration of < 27 ppm were found in the ICP-MS samples.

A UV-Vis spectrum of this blue solution showed two absorption bands at 410 and 582 nm, (Figure 10). These absorption bands are near identical in energy to the absorption bands of chromium (III) in aqueous solution.[19] A report by Drazic *et al.* on the degradation of chromium metal in sulfuric acid at pH 1 reports that the metal dissolves in H_2SO_4 to produce Cr(II) and Cr (III) ions in a 7:1 ratio, respectively.[20] Furthermore they reported that, during the formation of Cr(II) ions, hydrogen was produced (equation 1). From known transition metal chemistry it can also be assumed that Ni(II), Fe(II/III) and Mn(II) are all present in solution through the reaction with acid and the evolution of H_2, hence the hydrogen produced during irradiation of this acid sample (Table 11). Due to the absence of intense transitions in the visible spectrum of Fe(III) or Mn(II) in dilute acid, coupled with the lack of increased peak intensity of the 410 nm band which could be assigned to the overlap with the 400 nm Ni(II) transition, we can therefore assign the blue color of the solution to the presence of Cr(III). Presumably Cr(II) ions present in solution were oxidized to Cr(III) in the presence of oxygen, introduced when the inner stainless steel container was breached.[20] Figure 10 also shows the spectrum of the neat 3rd irradiated LEU sulfate solution (158 g L^{-1} uranium) for which there is no observed 582 nm transition that could be assigned to Cr(III), the 410 nm transition effectively obscured by the uranyl absorption. This strongly suggests that chromium (III) ions were not present in this irradiated LEU sulfate solution at anywhere close to the 325 ppm levels observed post irradiation of 0.1 mol L^{-1} H_2SO_4. This, in turn, indicates minimal corrosion of the steel inner container in the uranium sulfate solution. While we do have to consider that the 0.1 mol L^{-1} H_2SO_4 solution remained contained in the primary container longer than any of the irradiated LEU sulfate solutions there is still enough evidence to suggest that, by some mechanism, the presence of uranium suppresses corrosion.

$$Cr + 6\,H_2O + 2\,H^+ \rightarrow [Cr(H_2O)_6]^{2+} + H_2 \qquad (1)$$

3.3. Irradiated LEU Sulfate Samples

3.3.1 Analysis of the Irradiated Solutions

Uranium concentration pre- and post-irradiation for the three LEU sulfate solutions are shown in Tables 2 and 3 respectively. The concentrations were obtained using the UV-Vis spectrometry method described in section 2.3.3. The concentration measurement for each sample was undertaken in triplicate, except for the 3rd post-irradiation LEU sulfate solution which was undertaken only once (158 gU L^{-1}). The uranium concentration for the 1st and 3rd LEU sulfate solutions appeared to increase slightly post-irradiation, while for the 2nd irradiated sample the uranium concentration was essentially the same pre- and post- irradiation. For the 3rd LEU sulfate target solution sample the fact that only one uranium concentration measurement was made on the post-irradiation sample could account for the apparent increase in uranium concentration. However, for the 1st sample a concentration change from 150(±1) gU L^{-1} to 156(±1) gU L^{-1} post-irradiation is somewhat more difficult to explain. Water radiolysis would have a negligible effect on solution volume at the extent of irradiation that could be achieved in a Target 4 experiment. As the pre-irradiation UV-vis measurement yielded a uranium concentration that was is very good agreement with the Davis-Gray analysis (150.3 gU L^{-1}, section 2.3.4) then it is unlikely that this value is low. Perhaps an additional systematic pipetting error was introduced into the post-irradiation uranium analysis measurement, which in turn could indicate that the UV-Vis analysis technique requires some refinement. Nevertheless, observed differences in pre- and post-irradiation uranium concentration were all below 4 % which is reflected in the solution density measurements which were essentially unchanged pre- and post-irradiation (Table 7).

The pH of the three uranium target solutions were recorded pre- and post-irradiation (Table 7). They did not fluctuate beyond pH 1.0-1.2 for any of the 6 recorded measurements, indicating that there had been no significant change in acidity. This is unsurprising; H_2SO_4 should be relatively stable to radiolysis,[7] especially at the low extent of fission product production levels that could be obtained in these Target four experiments.

3.3.2. Sample Irradiation and Production Activities

The length of irradiation for the 1st, 2nd, and 3rd LEU samples were 6.0, 7.0 and 6.4 hours, respectively. End of beam (EOB) for the 1st, 2nd, and 3rd irradiations were 346.1326 (year 2012), 9.9278 (year 2013), and 28.0694 (year 2013), respectively. Times are report as for Greenwich Meantime using the digital calendar in place of h, min & sec. EOB was the time irradiation ended for each sample. Production activities for all three irradiated LEU sulfate solutions were measured by gamma spectroscopy at the

TA48 count room, both on 5.0 and 1.25 mL samples of solution (accurately measured). The 1.25 mL samples were diluted with 3.75 mL of 0.1 mol L^{-1} H_2SO_4 to make up to 5 mL volume. Samples were analyzed at different times after EOB, with short half-life radioisotopes usually yielding better count data when the measurement was undertaken close to EOB. Conversely, longer lived radioisotopes often yielded better count data when most of the shorter lived radioisotope activity had decayed, allowing longer count times.

The main radioisotopes generated during irradiation and their activities for all three irradiated LEU sulfate solutions at EOB (or at a fixed time after EOB) are summarized in Figure 11. This figure clearly shows greater radioisotope production for all the isotopes analyzed for the 3rd irradiation, followed by 1st and finally the 2nd. In each case *ca*. 1 mCi of ^{99}Mo was produced.

3.3.2.1. ^{99}Mo

^{99}Mo (half-life 2.7 days) production values were obtained using both the 181 KeV (Table 13) and 740 KeV (Table 14) transitions, with the data calculated back to EOB. The activity values obtained for both transitions are comparable for the analysis of each of the three irradiated samples, and are in good agreement with the 1 mCi of ^{99}Mo targeted production values.

3.3.2.2. $^{131/133}$I

^{131}I (half-life 8.02 days) production values for the three irradiated LEU sulfate solutions at EOB and 72 hours after EOB are shown in Table 15. Values were corrected to 72 hours after EOB for each irradiation in order to leave enough time for > 99 % ingrowth of ^{131}I from $^{131/131m}$Te (half-lives, ^{131}Te = 25 min and ^{131m}Te = 30 hours). The values obtained 72 hours after EOB were 121(1), 108(1) and 135(1) µCi for the 1st, 2nd, and 3rd irradiations, respectively. These values were in relatively good agreement with the calculated production value of 125 µCi 72 hours after EOB, assuming production of 1 mCi ^{99}Mo at EOB. A more detailed analysis of the ^{131}I data, relating directly to actual ^{99}Mo production values (section 3.3.2.1.), would indicate that the observed ^{131}I production values were slightly lower than expected. This can be accounted for through the loss of volatile iodine (I_2) prior to the gamma spectroscopy measurements. ^{133}I (half-life 20.8 hours) gamma spectroscopy results had large percent errors, and some currently unexplainable inconsistencies in activities for different samples. This is probably a combination of the short half-life and interference with other isotope gamma transitions at the 530 keV energy. Additional detailed analysis would be required to attempt to process the ^{133}I data further.

3.3.2.3. ^{239}Np and ^{143}Ce,

The production values for ^{239}Np (half-life 2.3 days) and ^{143}Ce (half-life 33 hours), were calculated to EOB and are shown in Tables 16 (^{239}Np) and Table 17 (^{143}Ce). The production values obtained for ^{239}Np are somewhat lower than the calculated value of 2420 µCi, for the production of 1000 µCi ^{99}Mo at EOB. For ^{143}Ce, the calculated production value was 1750 µCi at EOB (for 1000 µCi of ^{99}Mo) and it would appear that there is a slightly higher ratio of ^{143}Ce:^{99}Mo obtained through the analyzed gamma spectroscopy data (*ca.* 10 % more ^{143}Ce). With both ^{239}Np and ^{143}Ce it is not yet clear what could be causing the apparent discrepancy between the observed and calculated activities, but in terms of analyzing the subsequent separation chemistry data this was not significant.

3.3.2.4. ^{141}Ce, ^{95}Zr, ^{140}Ba, ^{147}Nd and ^{103}Ru

The production values for the relative longer lived radioisotopes (half-lives ranging from 10.9 days for ^{147}Nd to 64 days for ^{95}Zr) are shown in Table 18 (^{141}Ce), Table 19 (^{95}Zr), Table 20 (^{140}Ba), Table 21 (^{147}Nd) and Table 22 (^{103}Ru). In the time scale of these experiments the half-lives of these longer lived isotopes, coupled with poor binding to titania, were sufficiently long for there to be significant carry-over with the recycled irradiated fuel for the 2nd and 3rd irradiations. The only exception was ^{95}Zr which does very effectively bind to titania. All of the separation chemistry results are discussed in more detail in sections 3.3.3 and 3.3.4.

The calculated production values for ^{141}Ce (78 µCi, EOB) ^{95}Zr (45 µCi, 24 hrs after EOB), ^{103}Ru, (34.5 µCi, EOB) and ^{140}Ba, (219 µCi, EOB) for 1000 uCi produced ^{99}Mo agree well with the experimentally obtained values. This agreement is all the more apparent if these calculated values are scaled with the experimentally obtained ^{99}Mo production values. For ^{147}Nd, the experimentally obtained production values for the 1st and 3rd irradiations appear to be significantly higher that the calculated value (76 µCi 72 hours after EOB). However with good $^{141/143}$Ce gamma spectroscopy data providing data on the lanthanides there was no need to analyze for ^{147}Nd for the subsequent separation chemistry.

3.3.2.5. ^{105}Rh, ^{97}Zr and ^{140}La

The ^{105}Rh (half-life 35.4 hour) and ^{97}Zr (half-life of 16.9 hours) production values varied between irradiations and had significantly large % errors. Clearly a more detailed analysis of the gamma spectroscopy data would be needed to obtain useful production values for ^{105}Rh. For ^{97}Zr there is the close proximity of the main gamma transition at 757 keV with the ^{99}Mo transition at 740 keV, but the production values could often be used to confirm good activity balance for subsequent batch and

column separation data. ^{140}La (half-life 1.7 days) is the β-decay daughter of ^{140}Ba, with a 12.7 days half-life and thus no detail analysis was performed on this isotope.

3.3.3 First Irradiation – Batch Separation Chemistry

Previously, we have undertaken multiple batch distribution experiments with irradiated uranium samples, which revealed excellent binding of ^{99}Mo to the titania (TiO_2) sorbent.[10] In the Target Four runs, batch separation experiments were performed only on the 1st irradiated 150(1) g L^{-1} LEU sulfate solution, mainly to confirm that ^{99}Mo would bind to titania (as previously observed) and could then be stripped into the same 0.1 mol L^{-1} NaOH basic solution that was to be used for the column separation experiments (section 3.3.4.). If ^{99}Mo was successfully recovered then it would provide strong evidence that there was no reduction from Mo(VI) to Mo(IV), which would likely irreversibly bind to titania, and would provide good evidence that the column separation chemistry should work successfully. Triplicate batch experiments were performed for this irradiated solution. All of the batch contact experiments were performed for 22.5 hours at 70 °C, with constant sample shaking, the aim being to ensure that equilibria had been reached. Gamma spectroscopy data for the control sample (irradiated solution prior to contact with TiO_2), irradiated uranium solution post-contact and 0.1 mol L^{-1} NaOH strip post-contact are shown in Table 23. The TiO_2 sorbent from sample 3 was combined with 5.0 mL of H_2O and submitted for gamma spectrometry analysis (again, see Table 23). The titania sorbent was originally white, but turned yellow after separation as previously observed.[10] Distribution coefficient (kd) values for ^{97}Zr, ^{103}Ru and ^{99}Mo, in irradiated LEU sulfate solution post-contact, are shown in Table 24. Kd values were calculated as described previously.[9,21]

3.3.3.1. ^{99}Mo Batch Separation Chemistry

In previous batch separation experiments no ^{99}Mo activity was observed in the uranium fraction and the ^{99}Mo recovery was > 90% using 1 mol L^{-1} NH_4OH as the strip solution.[9] In this case, analysis of the uranium and base fractions revealed < than 9% of ^{99}Mo remained in the uranium fraction post-contact and that by using 0.1 mol L^{-1} NaOH as the strip solution it was possible to recover > than 88% of the ^{99}Mo bound to the titania sorbent (Table 23). Good activity balances were obtained using both ^{99}Mo gamma transitions, 181 and 740 keV. Analysis of the titania sorbent revealed that, for this set of batch separation experiment, no ^{99}Mo was left bound to the sorbent post-contact with base. In contrast, our previous batch separation experiments showed that 2 – 4% of the ^{99}Mo could remain bound to the titania sorbent.[10] This may indicate that either NaOH is a better ^{99}Mo stripping solution than NH_4OH, and/or that in the previous batch separation experiments some of the ^{99}Mo was reduced to (IV) making

it irreversibly bind to the titania sorbent, and/or that the higher temperature in which this set of control experiments was undertaken facilitated the stripping of all the bound ^{99}Mo. The subsequent irradiated uranium solution column experiments would reveal no detectable amounts of ^{99}Mo in the fractions containing uranium, > 94 % recovery of ^{99}Mo in 0.1 mol L^{-1} NaOH base fractions and no ^{99}Mo left bound to the sorbent (section 3.3.4.1.). It can thus be concluded that in the two batch experiments where observable ^{99}Mo activity remained in the irradiated uranium solution, post-contact with titania, separation equilibria had not been reached (perhaps due to inadequate mixing). This is reflected in the comparatively low K_d values for those two experiments (Table 24).

3.3.3.2. ^{131}I, ^{239}Np, $^{141/143}$Ce, ^{140}Ba, $^{95/97}$Zr and ^{103}Ru Batch Separation Chemistry

As previously observed, iodine behavior in the titania separation process for ^{99}Mo recovery from irradiated uranium solutions is complex.[10] In this set of batch experiments a fraction of the ^{131}I remained in the irradiated uranium solution post-contact (> 24%), a fraction was stripped into base (> 46%) and a fraction remained irreversibly bound to titania (13%). The poor activity balances are probably in part due to loss of volatile iodine (I_2) from the solutions. Previously we have also shown that ^{239}Np, $^{141/143}$Ce and ^{140}Ba do not bind to titania,[10] and these results confirm that finding. Excellent activity balances are observed for all four radioisotopes. Both ^{95}Zr and ^{97}Zr bind irreversibly to titania, with high K_d values (Table 24). Again, this is consistent with previous work.[10] The comparatively large measurement errors in the titania gamma spectroscopy measurement could be a contributing factor to the low activity balance in sample 3 for ^{97}Zr. We had not looked at ^{103}Ru binding to titania in previous irradiation experiments.[10] These batch experiments clearly show that a sizeable fraction of ^{103}Ru does not bind to titania (> 41%), resulting in low K_d values (Table 24). A comparable fraction of the ^{103}Ru does bind (48%), and remains irreversibly bound. Of most interest is the observation that between 5 – 6 % of the ^{103}Ru is stripped with 0.1 mol L^{-1} NaOH and would thus be a significant contaminant, along with ^{131}I, of the ^{99}Mo product.

3.3.4 Irradiated LEU Sulfate Samples – Column Separation Chemistry

After samples had been taken for gamma spectroscopy, batch separation experiments (1st irradiation only), iodine speciation experiments and uranium concentration measurements, the remaining irradiated uranium solutions (129 mL, 1st irradiation; 128 mL, 2nd irradiation; 136 mL; 3rd irradiation) were used for the column separation experiments, one experiment per irradiated uranium sulfate solution. A detailed description of the titania column separation chemistry, and associated apparatus, was provided in section 2.5.3. During the experiments 16 fractions of various volumes were collected for

the 1st and 2nd irradiated solutions while 15 fractions were collected for the 3rd irradiated solution. In each case the first fraction collected was a 'pre-uranium' fraction composed of a mixture of 0.1 mol L^{-1} H_2SO_4 and irradiated LEU sulfate solution, in which a lower uranium concentration sample was collected prior to collection of the second fraction which contained the bulk of the uranium solution. The third and fourth fractions were collected at the same time as the 1.0 mol L^{-1} H_2SO_4 acid wash was being pumped through the column, while the fifth and sixth fractions were being collected as the water wash was being pumped through the column. The remaining fractions were collected after the 0.1 mol L^{-1} NaOH solution has started to be pumped through the column. In practice it took several base fractions to completely neutralize the acid remaining bound/entrained within the column before the collected fractions became basic. While the 1st irradiated LEU solution contained only uranium that had previously been un-irradiated, the 2nd irradiated LEU solution contained the majority of the 1st irradiated solution (78 %) that had previously been passed through a titania column. In turn, the 3rd irradiated solution contained the majority of the 2nd irradiated solution (77 %) that had previously been passed through a titania column separation. Figures 12 – 14 show the column separation data for ^{99}Mo and ^{131}I, while Figures 15 –17 show the column separation data for LEU, ^{239}Np, ^{103}Ru, ^{105}Rh, ^{141}Ce, ^{143}Ce, ^{140}Ba, ^{132}Te, ^{95}Zr and ^{97}Zr. Tables 25 – 27 present the column separation data for all of the radioisotopes in the three irradiated solutions, while tables 4 – 6 show the uranium concentration measured in fractions 1 – 4 in the three irradiated solutions. Table 28 shows that volume of irradiated LEU sulfate fed through each column and the volume of 0.1 mol L^{-1} NaOH required to strip > 94 % ^{99}Mo.

3.3.4.1 ^{99}Mo Column Separation Chemistry

^{99}Mo column separation experiments yielded greater than 94% ^{99}Mo recovery in small volumes of base for the 1st and 2nd irradiations (9.3 and 9.7 mL). This confirms that the downscale separation worked, even when using recycle fuel (2nd irradiation). The larger volume (22.3 mL) of base in which > 94% of the ^{99}Mo could be recovered for the 3rd irradiation can be related to the fact that the column was stopped multiple times as part of a testing process designed to be more applicable with the subsequent Blue Room irradiation (70 mCi ^{99}Mo produced), and associated hot cell chemistry. Much lower ^{99}Mo activities were observed in the subsequent basic column fractions and the last collected low pH fraction prior to the column fractions becoming basic. Generally good ^{99}Mo activity balance was obtained, using both the 181 and 740 keV energies, for each column separation experiment. There was no observed breakthrough with the irradiated uranium solution, as seen in the batch separation experiment (section 3.3.3.1.), and no observed ^{99}Mo irreversibly bound to the titania sorbent post-column. The absence of ^{99}Mo activity in the uranium solution post-column separation, and irreversibly bound to the titania

sorbent suggests that extraction of ^{99}Mo using the titania column was more efficient than the ^{99}Mo separation in the batch experiments in section 3.3.3.1, and indeed in our previously reported batch separation experiments.[10]

3.3.4.2. ^{131}I Column Separation Chemistry

^{131}I activity data in the different column fractions is shown in Figures 12 – 14 and Tables 25 – 27. From both the batch separation chemistry experiments on the 1st irradiated solution (section 3.3.3.2.) and our previously published ^{131}I data,[10] we observed that ^{131}I had very complex separation chemistry behavior. In those previous experiments iodine partitioned between the acidic uranium and basic ^{99}Mo fractions, with evidence of some ^{131}I irreversibly binding to titania sorbent (along with indirect ingrowth through decay of bound ^{131m}Te). The Target 4 column separations data reveals even more complex ^{131}I behavior (Table 29). A proportion of the ^{131}I does not bind to the titania sorbent, remaining with the uranium product (8 – 24%); is stripped from the column with the 1.0 mol L^{-1} H_2SO_4/water washes (3 – 10%); is washed with 0.1 mol L^{-1} NaOH at pH < 11.7 (prior to column neutralization, 16 – 35%); is eluted with 0.1 mol L^{-1} NaOH at pH > 11.7 (41 – 55%); is irreversibly binding to the column (3 – 5%, Table 29). In addition, poor activity balance is indicative of loss of ^{131}I to the gas phase. Of most significance is the fact that more than 41% of the ^{131}I elutes with the ^{99}Mo product, where it will need to be removed through further ^{99}Mo product purification.[21] In the case of the SHINE ^{99}Mo production scheme further ^{99}Mo purification would occur through the ANL developed modifications to the CINTICHEM process.

3.3.4.3. ^{103}Ru Column Separation Chemistry

Significant proportions of the ^{103}Ru, 30 – 66%, passed through the titania columns for all three irradiated solutions without binding and were collected in the uranium column fractions (see Table 30). Between 22 – 43% of the ^{103}Ru remained irreversibly bound to the titania sorbent, with similar behavior also observed during the batch separation experiments (section 3.3.3.2.). Analysis of the basic fractions after ^{99}Mo decay for the 1st irradiation revealed that all the basic column fractions containing ^{103}Ru contaminant (Figure 15). This analysis was not performed for the 2nd and 3rd irradiations but it could probably be assumed that ^{103}Ru was also present in all the basic column fractions for these two separation experiments as well. Therefore a small (< 1%) but significant fraction of the ^{103}Ru will contaminate the ^{99}Mo product. In addition, comparing the distribution of ^{103}Ru between the column fractions for all three column separation experiments reveal significant differences. This is probably indicative of changes in Ru chemical speciation, most likely caused by changes in Ru oxidation state (III,

IV). Further studies may be required to determine if such differences have a major impact on how much ^{103}Ru is carried over with the ^{99}Mo product.

3.3.4.4. ^{132}Te Column Separation Chemistry

^{132}Te (half-life 3.2 days) has a major gamma transition at 228 keV. Unfortunately, ^{239}Np (half-life 2.4 days) also has a transitions at the same energy and thus far there has been no attempt to de-convolute the spectra to analyze for ^{132}Te in the presence of ^{239}Np. Removal of ^{239}Np in the first few column fractions was confirmed by the absence of the major transitions that was followed for ^{239}Np, 278 KeV, in the rest of the column fractions. The absence of ^{239}Np was also confirmed by the absence of additional ^{239}Np transitions (*e.g.* 106 KeV), and thus from column fraction 5 (1st and 3rd irradiation samples) and 6 (2nd irradiation sample) onwards the 228 keV transition could be used to quantify any ^{132}Te present. Analysis revealed that ^{132}Te was found in both the acidic and later basic fractions, see Figures 15 – 17, with some ^{132}Te also binding irreversibly to titania, Tables 25 – 27. Analysis of the basic fractions for the 1st irradiation revealed that ^{132}Te also contaminates the ^{99}Mo product (Figure 15). The 2nd and 3rd column experiments provided progressively less information on ^{132}Te activities in the basic fractions. This can be attributed to, at least in part, the progressively longer times between EOB and column separation for the three irradiations, and thus lower activities of ^{132}Te at count time.

3.3.4.5. $^{95/97}$Zr Column Separation Chemistry

No detectable amounts of $^{95/97}$Zr were observed in the ^{99}Mo product and in the bulk uranium fraction, thus no detectable Zr carried through with either the ^{99}Mo product or the uranium for recycle. The acid wash did strip some $^{95/97}$Zr from the column. This is significant, if Zr(IV) behaves like Pu(IV) then that provided evidence that some Pu (^{239}Pu, from decay of ^{239}Np) would strip from the column in acid, if present in the +IV oxidation state. The remaining $^{95/97}$Zr remains bound to the titania sorbent, even after washing with base. Good activity balances were generally obtained for each isotope.

3.3.4.6. Uranium, ^{239}Np, ^{140}Ba, ^{105}Rh and $^{141/143}$Ce Column Separation Chemistry

Column separation results for the three experiments show that uranium, ^{239}Np, ^{140}Ba, ^{105}Rh and $^{141/143}$Ce pass through the column without binding and that these radioisotopes are collected in the first few fractions as shown in Figures 15 – 17 and Tables 25 – 27. The uranium concentration (presented as µCi mL^{-1}) for fractions 1 through 4 were calculated using the UV-vis technique described in the experimental section and their results are shown in Tables 4 –6. In each case the activity balance was very good. ^{105}Rh has a poor activity balance, a result of our current incomplete understanding of discrepancies in the gamma spectroscopy data (as previously described in the section 3.3.2.5.). However, it can still

clearly be seen that ^{105}Rh does not bind to titania sorbent. Many of these results could be predicted from our previous batch distribution data,[10] and from the batch distribution experiments performed for the first irradiation (3.3.3.2.).

3.3.5 Titania Sorbent Analysis

After the column separation experiments the columns were dismantled from the separation apparatus and the titanium sorbent poured out into a 20 mL glass vial as shown in Picture 3. The sorbent was combined with water and submitted for gamma spectrometry analysis. The list of isotopes bound to the sorbent and their activities are shown in Tables 25 – 27. As discussed previously (sections 3.3.4.2 to 3.3.4.5), $^{95/97}$Zr, ^{103}Ru, ^{132}Te and ^{131}I were all observed bound to titania. The titania sorbent looked the same for both the batch separation (section 3.3.3.) and the column separation (section 3.3.4.) experiments. The sorbent used in the batch separation and all three columns were originally white, but turned yellow after separation. Previous diffuse reflectance spectroscopy studies indicated the presence of two distinct broad band transitions in the visible region which could indicate the presence of $UO_2(OH)_2.xH_2O$, or partial titania decomposition to a more amorphous material.[10,22]

3.4 Iodine Speciation

Iodine speciation experiments,[23] followed by gamma spectroscopy analysis of ^{131}I, were characterized by poor activity balance (Tables 31 and Figure 18). This was particularly the case for the irradiated uranium solution after the 2nd sample irradiation. This could in part be attributed to loss of volatile iodine (as I_2) during the experiment. The speciation experiments were designed to separate and quantify the three most likely iodine species to be present in solution, I^-, I_2 and IO_3^-. In each of the three irradiated solution samples there was an increase in % of species present in solution along the series $I_2 < I^- < IO_3^-$, although it must be acknowledged that loss of I_2 to the gas phase has likely distorted these figures.

For the 3rd irradiated uranium solution iodine speciation measurements were also undertaken on three column fractions post irradiation; fraction 2 containing the bulk of the uranium; fraction 7, an acidic solution prior to elution of the alkaline fractions and fraction 9 which was the first basic fraction that also contained ^{99}Mo product (Table 32 and Figure 19). For fractions 2 and 7 the dominant iodine species was I_2, with IO_3^- also a significant species present in fraction 2. The alkaline fraction 9 solution had to be acidified by H_2SO_4 prior to extraction with chloroform which may have altered iodine speciation. However, if it is assumed that no change in speciation occurred on acidification, the speciation results for fraction 9 indicate that I^- was the dominant species, with some I_2 and no observed IO_3^-. This would indicate that I^- is the dominant species of ^{131}I contaminating the ^{99}Mo product.

3.5 Gas Analysis

The collected gas produced during the three LEU sulfate solution irradiations is shown in Table 10. The amounts of gas pressure collected after the first and second irradiations were almost the same, 284 and 292 torr. The gas pressure collected for the third irradiation was significantly higher, 409 torr. Gas analysis (by mass spectrometry) of the collected gas samples indicated *c.a.* 4:1 hydrogen to oxygen molar ratios (Table 11). Back calculating the observed % ratios of H_2, O_2 and Ar in the post-irradiation gas fractions to predict pressure increase during the three LEU sulfate solution irradiations indicated that pressures of 350, 300 and 300 torr should be observed for the 1st, 2nd and 3rd irradiations.

While there is obviously some scatter in the obtained data it is clear that during irradiation there was radiolysis of water which introduced H_2 and O_2 into the gas phase, thus increasing the gas pressure in the stainless steel inner containers holding the three irradiated samples. The radiolysis of water should produce a 2:1 ratio of hydrogen to oxygen and there are a number of factors which could result in the experimentally observed ratio of *ca.* 4:1. Firstly, due to safety constraints the mass spectrometry system could only be calibrated with 4 % H_2 in Ar whereas all the observed measurements were around 26-28 % H_2 in Ar/O_2. Thus the measured hydrogen values were significantly higher than the calibration point and there could be systematic errors introduced. While not a confirmed systematic error it should also be noted that there is the detection bias of the residual gas analyzer for lower molecular weight ions. This phenomenon is well-documented in the Stanford Research Systems manuals and instructions, and required a correction factor to account for this bias. In a standard 4 % H_2/Ar mixture, the RGA found an H_2 percentage of 8.7 % (taken by dividing the partial pressure of H_2 by the sum of the partial pressures), while in a 6 % O_2/Ar mixture the oxygen pressure detected by the RGA was 3 %. By dividing 4 % (expected) H_2/Ar mixture by 8.7 % (observed) a correction factor of 0.46 for hydrogen was obtained. Similarly, the correction factor obtained for oxygen was 2.0. These correction factors were used to calculate the percentages of hydrogen and oxygen in the irradiated gas samples.

There are also chemical considerations that could contribute to an H_2 to O_2 ratio of greater than 2:1, including increased solubility of O_2 (*vs.* H_2) in aqueous solution, corrosion of stainless steel and peroxide formation. Previously we have shown that corrosion of stainless steel leads to the production of hydrogen gas, and the introduction of transition metal cations into solution (section 3.2). While solution UV-vis spectroscopy analysis indicated far less corrosion in the three irradiated uranium solutions any corrosion would release hydrogen into the gas phase. Finally, peroxide formation after radiolysis would lead only to the release of hydrogen gas and there could have been peroxide generation below the

concentration required for the precipitation of uranyl peroxide (no precipitates were observed in any of the three irradiated LEU solutions).

4. Impact of Recycling Low Enriched Uranium in Target Solutions

As previously stated, the 2nd irradiation used 78% of the fuel from the 1st irradiation column separation and the 3rd irradiation used 77% of the fuel from the 2nd irradiation column separation. Comparing the gamma spectroscopy data for all three fractions 2's from the three column separation experiments, the bulk uranium fractions, allows the most direct comparison of radioisotope build up during fuel recycle (see Table 33). Obviously the shorter lived radioisotopes (^{105}Rh, ^{143}Ce, and ^{239}Np) will not accumulate to a great extent from one radiation to the next, but daughter radioisotopes may, for example ^{239}Pu from β decay of ^{239}Np. In contrast, the longer lived radioisotopes (^{103}Ru, ^{140}Ba, ^{141}Ce, and ^{147}Nd) do accumulate and these are the major contributors to the fission product activity in the recycled LEU sulfate fuel.

5. Conclusion

New sample containment methods, a new capability for accessing neutron irradiation at LANSCE, and separation apparatus applicable to ^{99}Mo recovery from irradiated LEU sulfate solution have all been developed. Both the stainless steel sample containment and irradiation capabilities were first successfully tested using water and sulfuric acid as the fill solutions. The new capabilities have been applied to a technical demonstration of ^{99}Mo recovery from three separate irradiated LEU sulfate solution using a titania column separation process. The titania column separations were highly successful, with a high % recovery of ^{99}Mo in a low volume of basic (0.1 M NaOH) solution during separation from the 1st and 2nd irradiated LEU solutions. The high volume of NaOH solution required to recover almost all the ^{99}Mo after the 3rd sample irradiation can be attributed to testing of the elution process for adaption of the separation procedure for hot cell operation. The 2nd and 3rd irradiated solutions contained LEU sulfate fuel recovered from the column separation processes for the 1st and 2nd irradiations respectively. At this extent of irradiation these results show that once the ^{99}Mo has been removed from the uranium sulfate fuel, the fuel can be recycled to produce more ^{99}Mo. Analysis of the ^{99}Mo product, post-titania column separation, indicated that ^{131}I, ^{132}Te & ^{103}Ru were all significant contaminants. A more detailed analysis of ^{131}I speciation revealed complex chemistry, with iodine present in all solution fractions post-column separation, and entering the gas phase. Analysis of the bulk uranium fractions post-column separation process indicated that longer lived isotopes, including ^{103}Ru

and ^{141}Ce, would start to build up in the LEU sulfate target solutions after multiple recycles. Additionally, the refinement of a simple spectroscopic technique for determining uranium concentration allowed for analysis of uranium target solutions and solution fractions from the column separations. Analysis of both the solution and gas phases' post–irradiation indicated observable corrosion of the stainless steel when 0.1 mol L^{-1} H_2SO_4 was irradiated, but significantly less corrosion when LEU sulfate pH 1 Target solutions were irradiated. This would indicate that the presence of uranyl sulfate in solution inhibits corrosion. Finally, post-irradiation gas analysis of the three irradiated LEU sulfate solutions indicated a build-up of gas pressure due to the radiolysis of water, with several factors likely contributing to the observed higher ratio of H_2 to O_2 in the gas phase *vs.* the expected ratio for water radiolysis (4:1 *vs.* 2:1).

6. References

1. Szymanski, J.J. and Staples, P., Ensuring a Reliable Supply of Medical Radioisotopes. **2012**. http://www.whitehouse.gov/blog/2012/03/27/ensuring-reliable-supply-medical-radioisotopes.
2. Reed, W. G.; Turkevich, A. Uranium-235 Thermal Neutron Fission Yields. *Physical Review*, **1953**, 92(6), 1473 – 1481.
3. Non-HEU Production Technologies for Molybdenum-99 and Technetium-99m. **2013** IAEA Nuclear Energy Series No. NF-T-5.4.
4. Service, R.F. Scrambling to Close the Isotope Gap. *Science* **2010**, 331, 277 – 279.
5. Medical Isotope Production Without Enriched Uranium. The National Academies Press, Washington DC, **2009**.
6. SHINE: Technology and Progress. Mo-99 2013 Topical Meeting on Molybdenum-99 Technology Development. Chicago IL, **2013**. http://mo99.ne.anl.gov
7. Homogenous aqueous solution nuclear reactors for the production of Mo-99 and other short lived radioisotopes. IAEA-TECDOC-1601, IAEA Vienna, Sept. **2008**. a) Stepinski, D.C.; Gelis, A.V.; Gentner, P.; Bakel, A.J.; Vandegrift, G,V. 73-80. b) Baranaev, Yu. D.; Nerozin, N.A.; Pivovarov, V.A.; Smetanin, E.Ya. 49-64.
8. Betenekov, N. D.; Denisov, E. I.; Nedobukh, T. A.; Sharygin, I. M. Inorganic Sorbent for molybdenum-99 extraction from irradiated uranium solutions and its method of use, World Patent W02001053205.
9. a) Youker, A. J.; Chung. P. L.; Tkac, P.; Quigley, k. J.; Makarashvili, V.; Bowers, D. I.; Chemerisov, S. D.; Vandegrift, G. F. Mo-99 2011 – Molybdenum-99 Topical Meeting, Santa Fe, NM, 2011. b) Youker, A.J.; Chemerisov, S,D.; Kalensky, M.; Tkac, P.; Bowers, D.L.; Vandegrift, G.F. A Solution-

Based Approach for Mo-99 Production: Considerations for Nitrate versus Sulfate Media. *Science & Technology of Nuclear Installations* **2013**, 2013, ID 402570. c) Ling, L.; Chung, P.L.; Youker, A.; Stepinski, D.C.; Vandegrift, G.F.; Wang, N.H. Capture chromatography for Mo-99 recovery from uranyl sulfate solutions: Minimum-column-volume design method. *J. Chromatogr. A* **2013**, 1309, 1-14.

10. a) Dale, E. G.; Dalmas, A. D.; Gallegos, J. M.; Jackman, R. K.; Kelsey, T. C.; May, I.; Reilly, D. S.; Stange, M. G. Mo-99 Separation from High-Concentration Irradiated Uranium Nitrate and Uranium Sulfate Solutions. *Ind. & Eng. Chem. Res*, **2012**, 51, 13319-13322. b) Anderson, A.S.; Bach, H.; Boland, K.S.; Copping, R.; Dale, G.E.; Dalmas, D.A.; Gallegos, M.J.; Jackman, K.R.; Kelsey (IV), C.T.; Lovato, L.I.; Janicke, M.; May, I.; Reilly, S.D.; Taw, F.L.; Wolfsberg, L.E. Mo-99 Separation and Gas Analysis from Irradiated Uranium Nitrate and Uranium Sulfate Solutions (Blue Room Experiment – January 2012), LA-UR-12-21346.

11. Anderson, S. A.; Bitteker, L. J.; Copping, R.; Dale, E. G.; Dalmas, D. A.; Gallegos, J. M.; Garcia, E.; Kelsey IV, T. C.; May, I.; Reilly, D. S.; Rios, D.; Stephens, H. F.; Taw L. F.; Woloshun, K. A Technical Demonstration of the Initial Stage of Mo-99 Recovery from a Low Enriched Uranium Sulfate Solution. Mo-99 2013 Topical Meeting on Molybdenum-99 Technological Development. Chicago, IL. **2013**. http://mo99.ne.anl.gov

12. Vopálka, D.; Štamberg, K.; Motl, A.; Drtinová, B. The study of the speciation of uranyl-sulphate complexes by UV-vis absorption spectra decomposition, *J. Radioanal. Nucl. Chem*. **2010**, 286, 681-686.

13. a) Denning, R. G. Electronic structure and bonding in actinyl ions and their analogs, *J. Phys. Chem. A.* **2007**, 111, 4125-4143. (b) Gorllerw. C; Vanquick. L.G. Coupling schemes in uranyl complexes, *Journal of Chemical Physics.* **1972**, 57, 1436-1440. (c) Hennig, C.; Schmeide, K.; Brendler, V.; Moll, H.; Tsushima, S.; Scheinost, A. C. EXAFS investigation of U(VI), U(IV), and Th(IV) sulfato complexes in aqueous solution, *Inorg. Chem.* **2007**, 46, 5882-5892. (d) De Houwer, S.; Gorller-Walrand, C. Influence of complex formation on the electronic structure of uranyl, *J. Alloy. Compd*. **2001**, 323, 683-687. (e) Ikeda-Ohno, A.; Hennig, C.; Tsushima, S.; Scheinost, A. C.; Bernhard, G.; Yaita, T. Speciation and Structural Study of U(IV) and -(VI) in Perchloric and Nitric Acid Solutions, *Inorg. Chem.* **2009**, 48, 7201-7210. (f) Hennig, C.; Ikeda, A.; Schmeide, K.; Brendler, V.; Moll, H.; Tsushima, S.; Scheinost, A. C.; Skanthakumar, S.; Wilson, R.; Soderholm, L.; Servaes, K.; Gorrler-Walrand, C.; Van Deun, R. The relationship of monodentate

and bidentate coordinated uranium(VI) sulfate in aqueous solution, *Radiochim. Acta* **2008**, 96, 607-611.

14. Ginosar, M. D.; Rollins, W. H.; Petkovic, M. L.; Burch, M. J.; Rush, J. M. High-temperature sulfuric acid decomposition over complex metal oxide catalysts, *Int. J. Hydrogen Energy*, **2009**, 34, 4065 – 4073.
15. a) Burneau, D. N.; Tazi, M.; Bouzat, G. Raman spectroscopic determination of equilibrium constants of uranyl complexes in aqueous solutions,' *Talanta* **1992**, 39, 743-748. (b) Volod'ko, V. L.; Sabilo, V. K. Raman spectra of solutions of uranyl compounds. *Zhurnal Prikladnoi Spektroskipii* **1966**, 4, 52-57. (c) Woodward, A. L.; Horner, G. R. Changes in the Raman spectram of sulfuric acid on dilution. *Proc. Royal Soc. London, Series A*, Containing papers of mathematical and physical character, **1934**, 144, 129-143. (d) Aksenenko, M. V.; Murav'ev, S. N.; Taranenko, S. G. Raman scattering study in nitric-acid solutions. *J. Appl. Spectrosc*, **1986**, 44, 70-72.
16. Davies, W.; Gray, W. A rapid and specific titration method for the precise determination of uranium using iron(II) sulphate as reductant. *Talanta* **1964**, 11, 1203 – 1211.
17. Kahn, M.; Wahl, C. A. Some Observations on the Chemical Behavior of Iodine at Low Concentrations, *J. Chem. Phys*. **1953**, 21(7), 1185 – 1189.
18. Bugorkov, S. S.; Krivokhatskii, S. A.; Petrzhak, A. K.; Skovorodkin, V. N. On the measurement of thermal-neutron fluxes and cadmium ratios from the activation of gold. *Atomnaya Energiya*, **1966**, 21(6), 508-509.
19. a) Thompson, M.; Connick, E. R. Hodrolytic Polymerization of Chromium (III). 1. Two Dimeric Species. *Inorg. Chem*. **1981**, 20, 2279 – 2285. (b) Stunzi, H.; Marty, W. Early Stages of the Hydrolysis of Chromium(II1) in Aqueous Solution. 1. Characterization of a Tetrameric Species. *Inorg. Chem*. **1983**, 22(15), 2145 – 2150. (c) Muñoz, E. L. B.; Rivera R. R.; Iturbe G. J. L.; Gutiérrez, O. M. T. *J. Mex. Chem. Soc.* **2011**, 55(3), 137 – 141.
20. Drazic, M. D.; Popic, P. J. Dissolution of Chromium in Sulfuric Acid. *J. Serb. Chem. Soc*. **2002**, 67(11), 777 – 782.
21. Management of Radioactive Waste from ^{99}Mo production, IAEA-TECDOC-1051, IAEA Vienna, 1988.
22. Randorn, C.; Irvine, J. T.; Robertson, P. Synthesis of visible-Light-Activated Yellow Amorphous TiO_2 Photocatalyst. *Int. J. Photo-energy*, **2008**, Article ID 426872.
23. Kelly P. G.; Timothy A. D. Development of a Novel Method for the Determination of Aqueous Inorganic ^{129}I Speciation. *Anal. Chem*. **2013**, 85, 4658 – 4665.

Pictures

Picture 1. Viking transport container containing a paint can, in which the sample was placed, surrounded by sorbent packaging material.

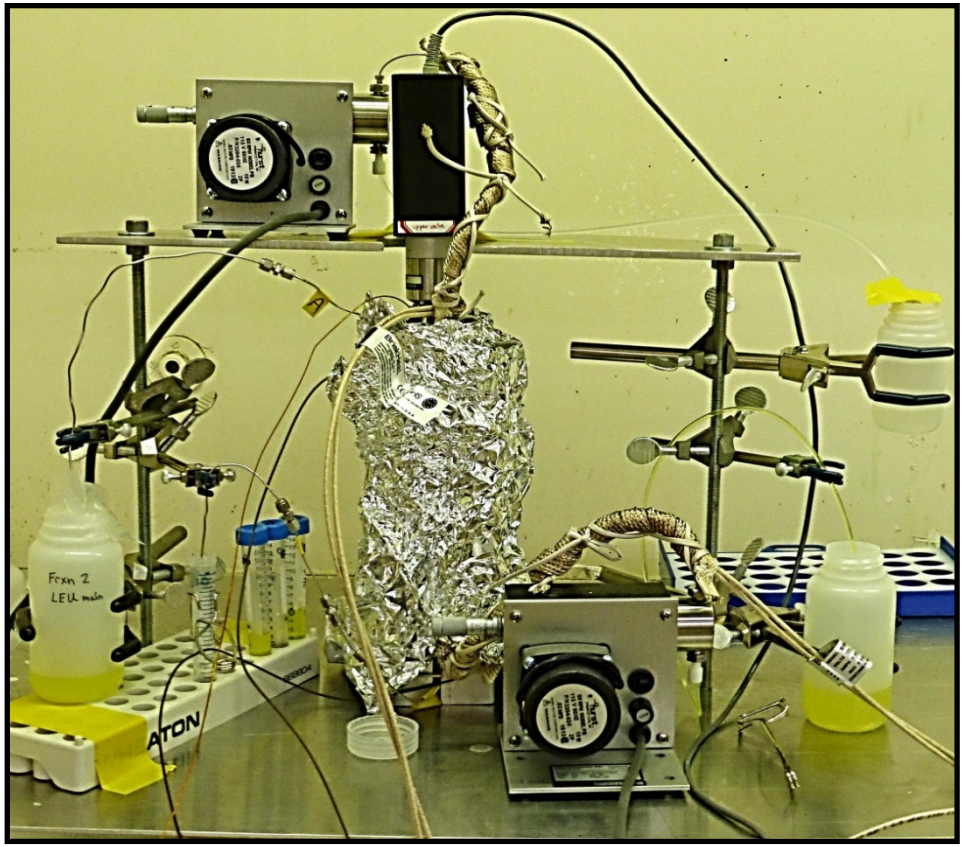

Picture 2. Column Separation Apparatus, the column itself obscured by the heating block covered with aluminum foil. The sample feed solutions are on the right and the sample collection vessels on the left. This picture was taken while the irradiated uranium solution was being pumped through the column.

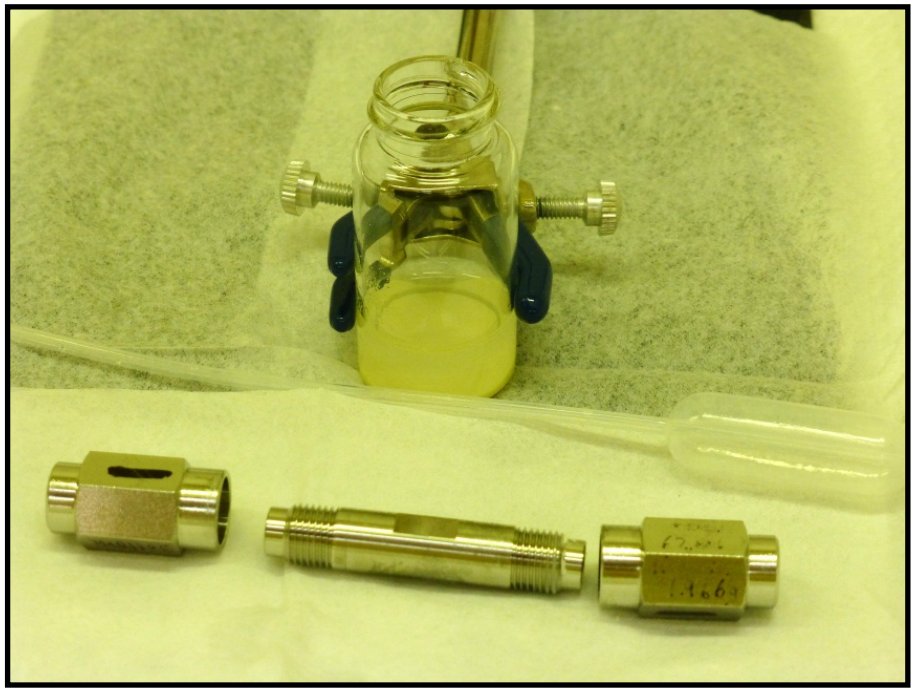

Picture 3. Column and post-separation titania sorbent.

Figures

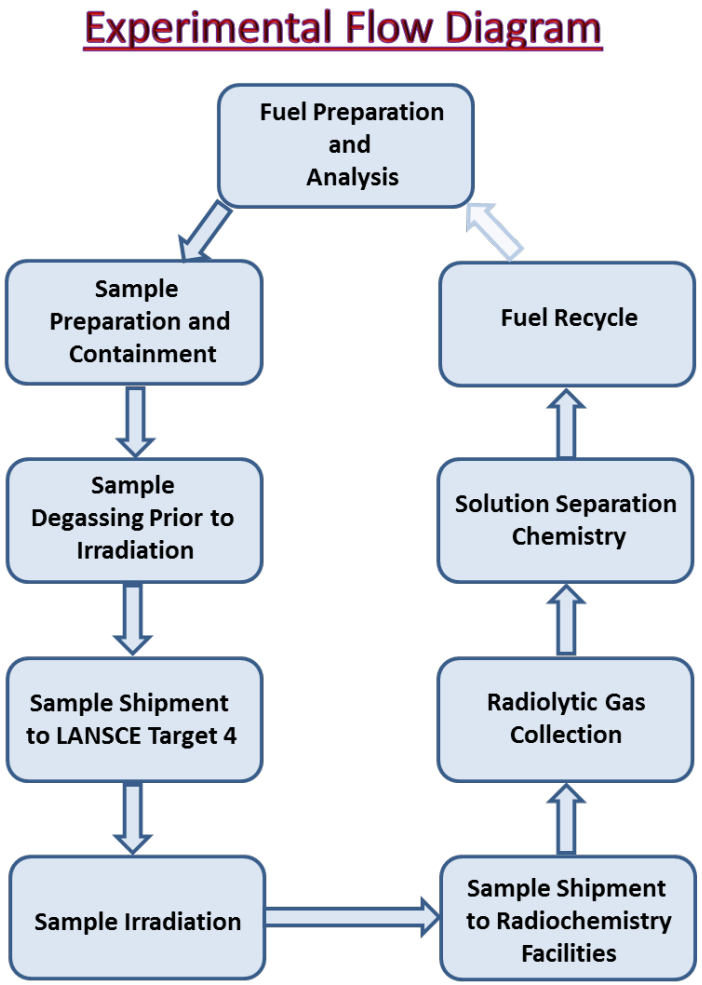

Figure 1. Flow diagram for the Target 4 experiments.

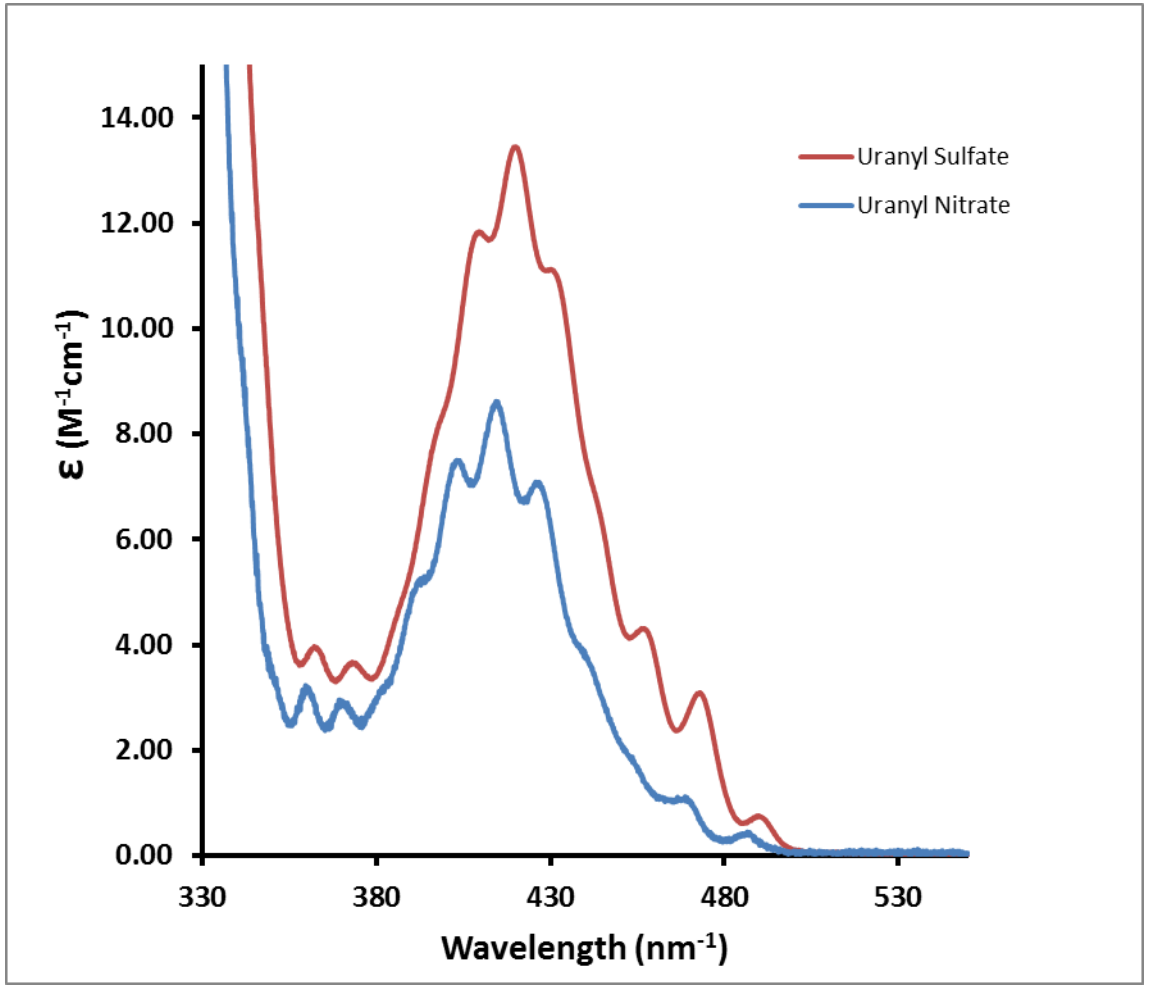

Figure 2. Absorption spectra of uranyl nitrate (blue) and uranyl sulfate (red) in 1 mol L^{-1} HNO_3 and 1 mol L^{-1} H_2SO_4 respectively. The λ_{max} and ε for uranyl nitrate and sulfate in these solutions are 414 and 420 nm, and 8.63 M^{-1} cm^{-1} and 13.65 M^{-1} cm^{-1}, respectively.

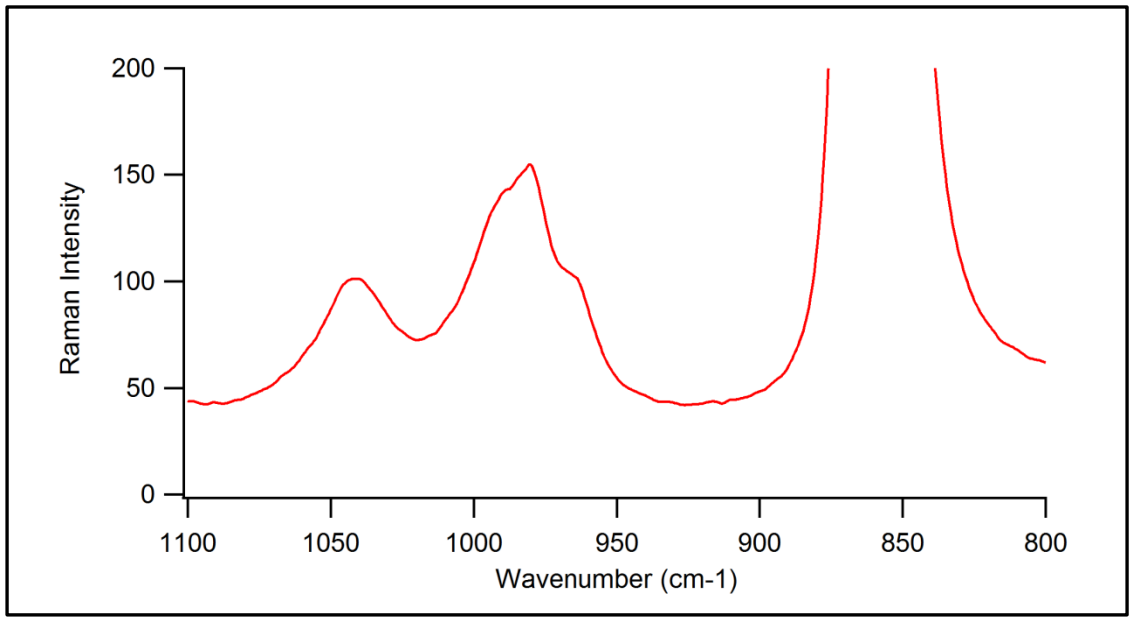

Figure 3. Raman spectrum of 150±1 gU L^{-1} LEU uranyl sulfate fuel at pH 1. The Raman bands centered at 856 and 976 cm^{-1} correspond to the $\nu_1(UO_2^{2+})$ and $\nu_1(SO_4^{2-})$ symmetric stretching frequencies, respectively. The 1045 cm^{-1} Raman band is the symmetric stretch vibration of the uncoordinated HSO_4^- $\nu_1(HSO_4^-)$. If present, the high intensity $\nu_1(NO_3^-)$ band of nitrate would be observed as a sharper band protruding at 1045 cm^{-1}.

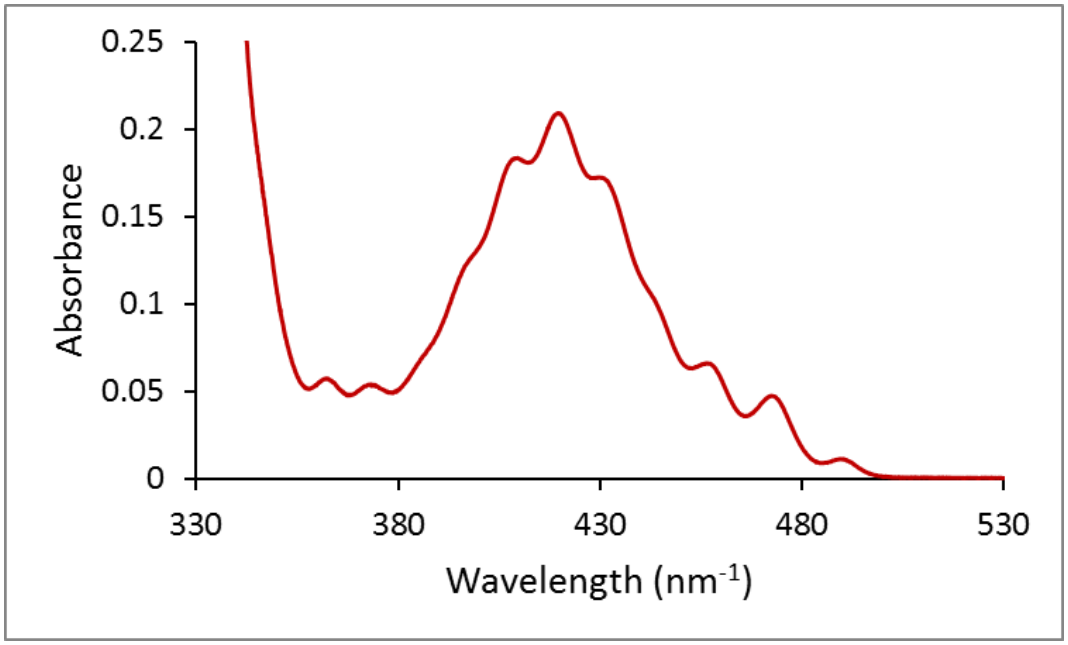

Figure 4. UV-vis absorption spectrum of the first assay of the pH 1.0 LEU uranyl sulfate target solution as uranyl(VI) sulfate spiked into 1 mol L^{-1} H_2SO_4. λ_{max} = 420 nm; A = 0.209. The uranium concentration was calculated using ε = 13.65(±2) L mol^{-1} cm^{-1} and determined to be 150 g L^{-1}.

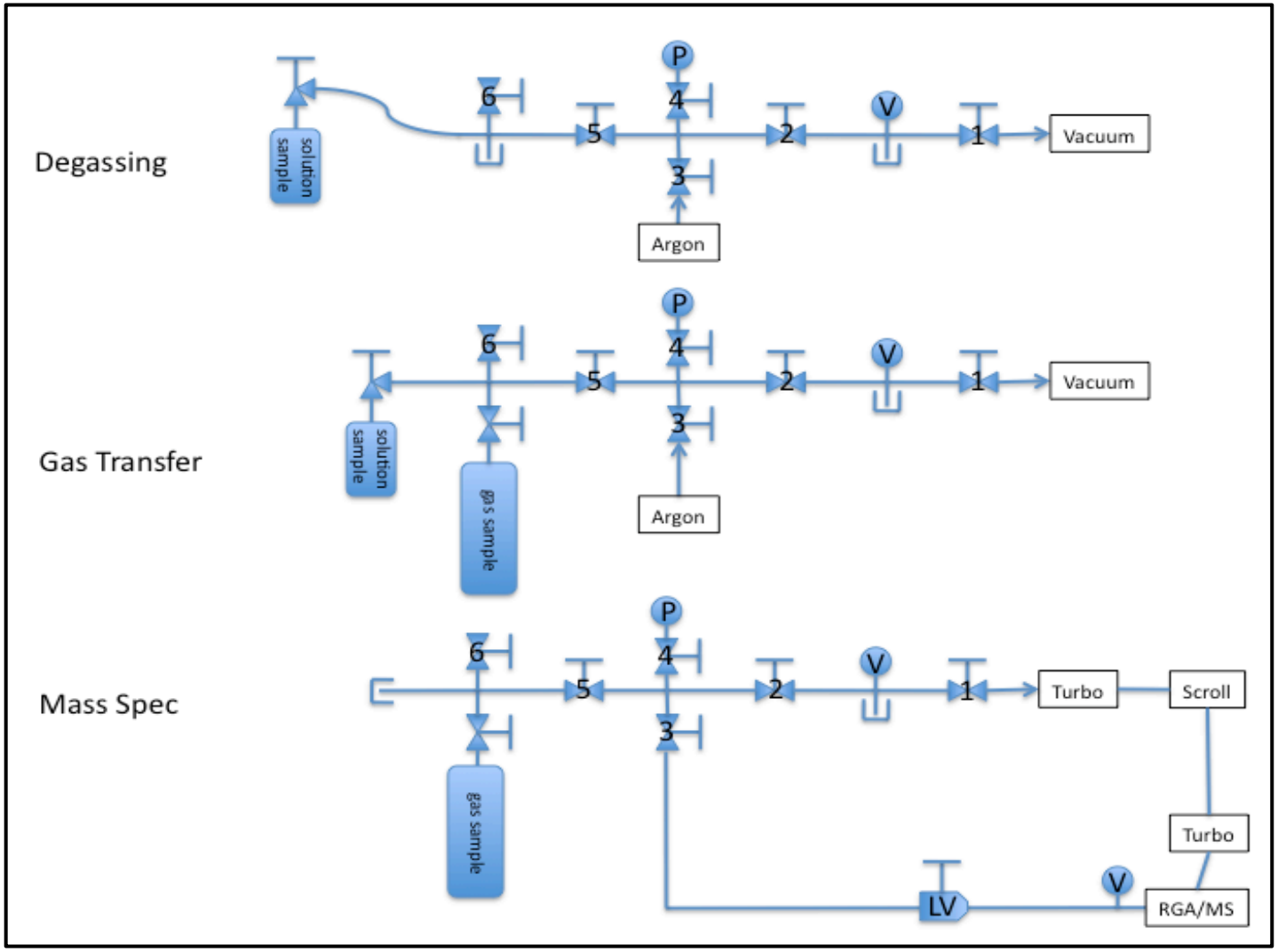

Figure 5. Schematic of the gas handling manifold with configurations for sample degassing, gas transfer, and mass spectrometry. P = pressure transducer; V = vacuum gauge; LV = variable rate leak valve; RGA/MS = residual gas analyzer/mass spectrometer. All fittings were Swagelok/Cajon VCR, except the "solution sample" (left) end of the manifold, which was a Swagelok tube fitting, and the vacuum fittings, which were KF (Klein Flange) or CF (conflat).

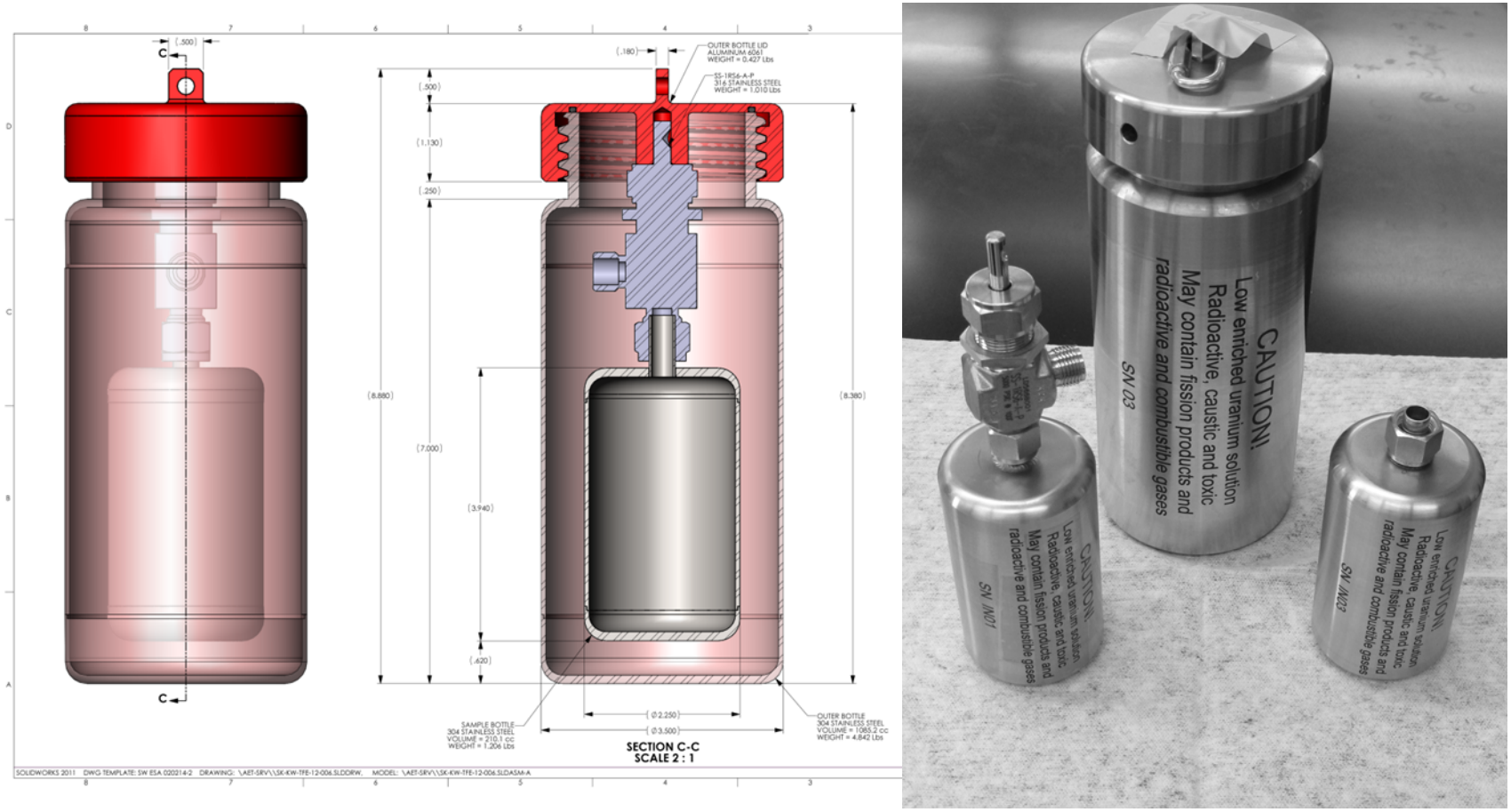

Figure 6. Drawing (left) and picture (right) of the Target 4 stainless steel sample containment.

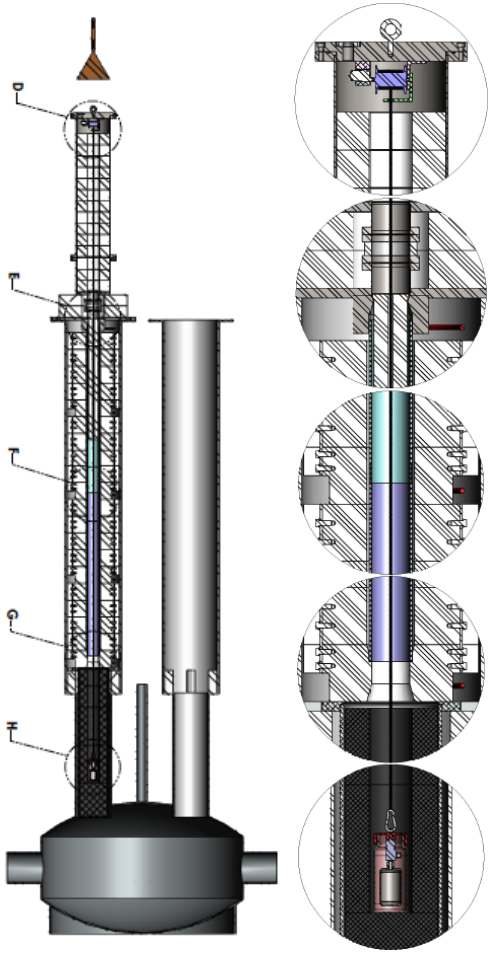

Figure 7. Diagram of the Target 4 irradiation insert installed at LANSCE with the sample in the lowered position.

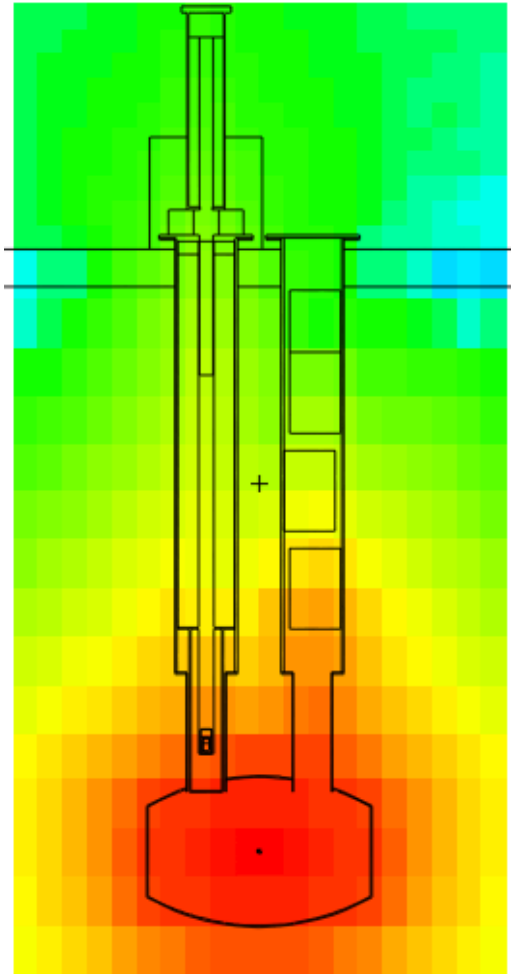

Figure 8. MCNPX model of Target 4 irradiation insert during irradiation. The yellow to green transition is at approximately 50 mrem/h/µA.

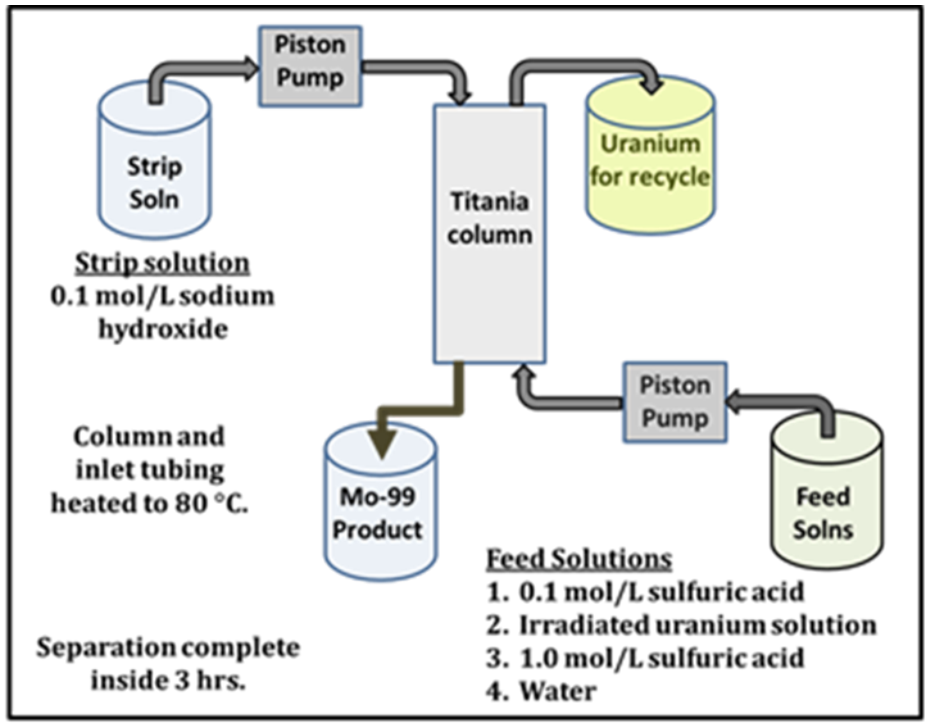

Figure 9. Schematic representation of the titania column separation process for ^{99}Mo recovery.

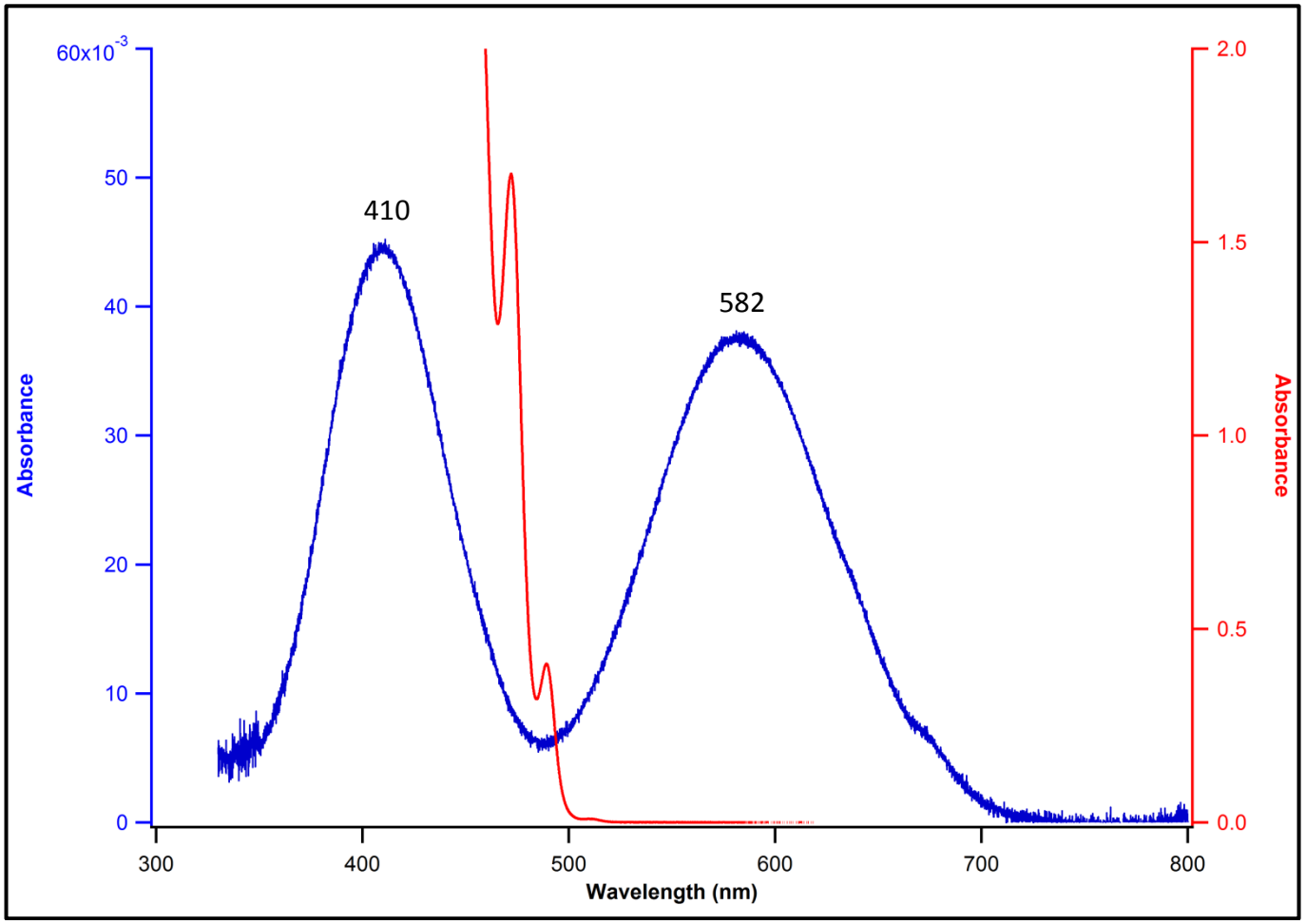

Figure 10. UV-vis absorption spectra of the irradiated 0.1 mol L^{-1} H_2SO_4 solution (blue, left axis) and the 3rd irradiated LEU sulfate solution (red, right axis) after the samples had remained in their respective stainless steel inner containers for 12 and 5 days. Solution pH's after irradiation were 1.0 and 1.2, respectively.

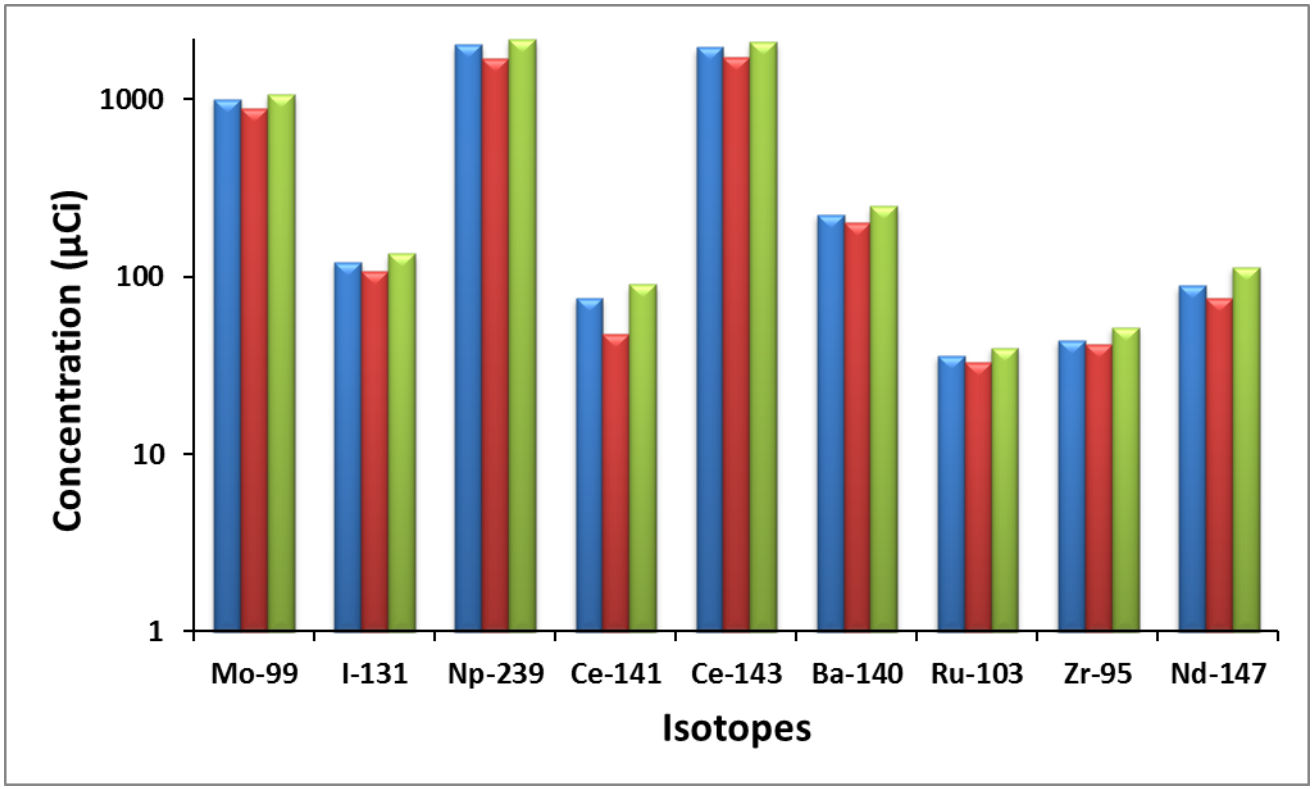

Figure 11. Isotopes produced, and their concentrations (µCi) in the 1st (blue), 2nd (red) and 3rd (green) irradiated LEU sulfate solutions. The ^{99}Mo, ^{239}Np, $^{141/143}$Ce, ^{140}Ba and ^{103}Ru activities were calculated back to EOB. ^{131}I and ^{147}Nd were calculated back to 72 hours after EOB. ^{95}Zr was calculated back to 24 hours after EOB.

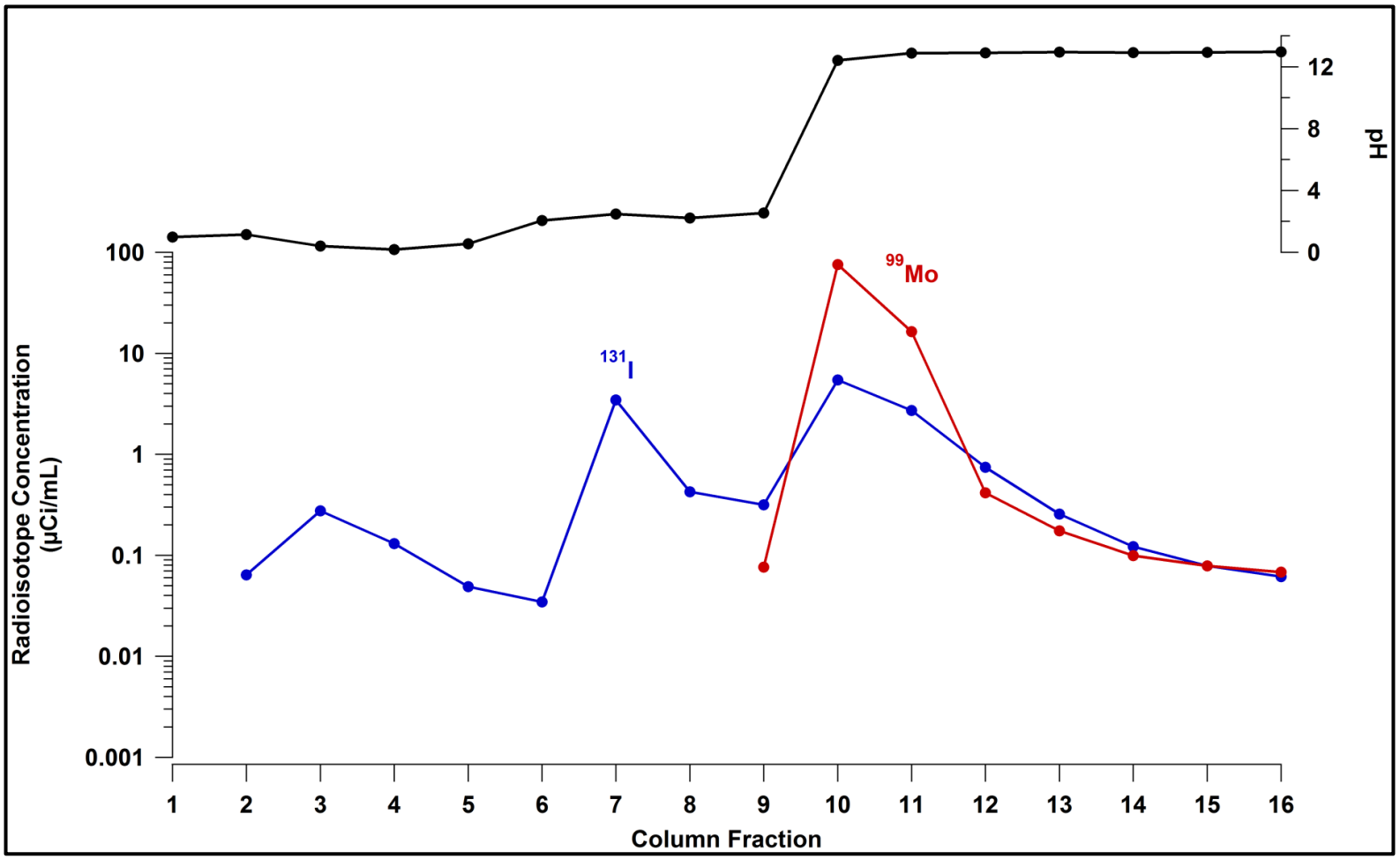

Figure 12. First irradiation LEU sulfate solution column separation data for ^{131}I and ^{99}Mo. EOB for this irradiation was 346.1326. Radioisotope concentrations were calculated to end of column time, 349.0208.

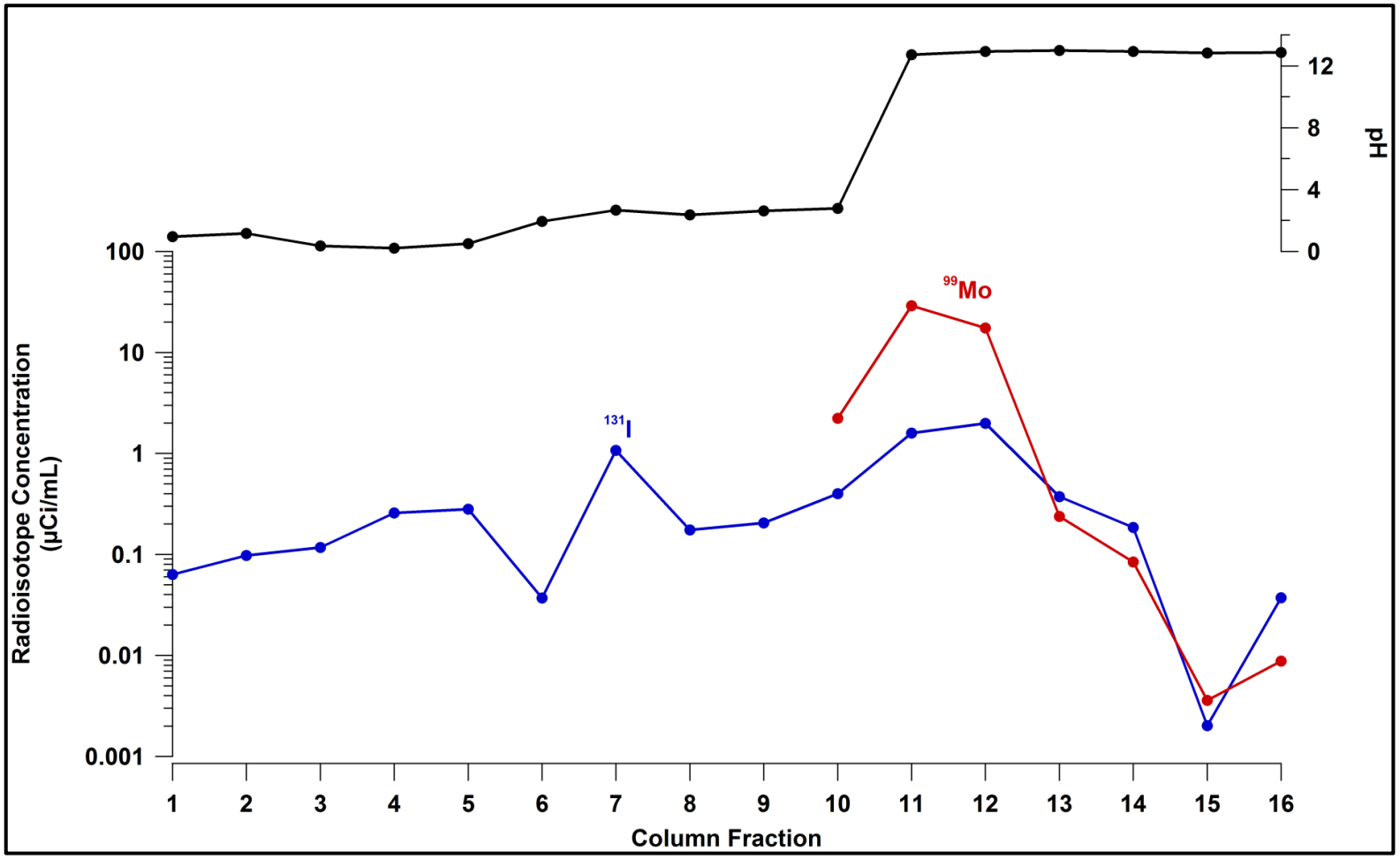

Figure 13. Second irradiation LEU sulfate solution column separation data for ^{131}I and ^{99}Mo. EOB for this irradiation was 9.9278. Radioisotope concentrations were calculated to end of column time, 14.9076.

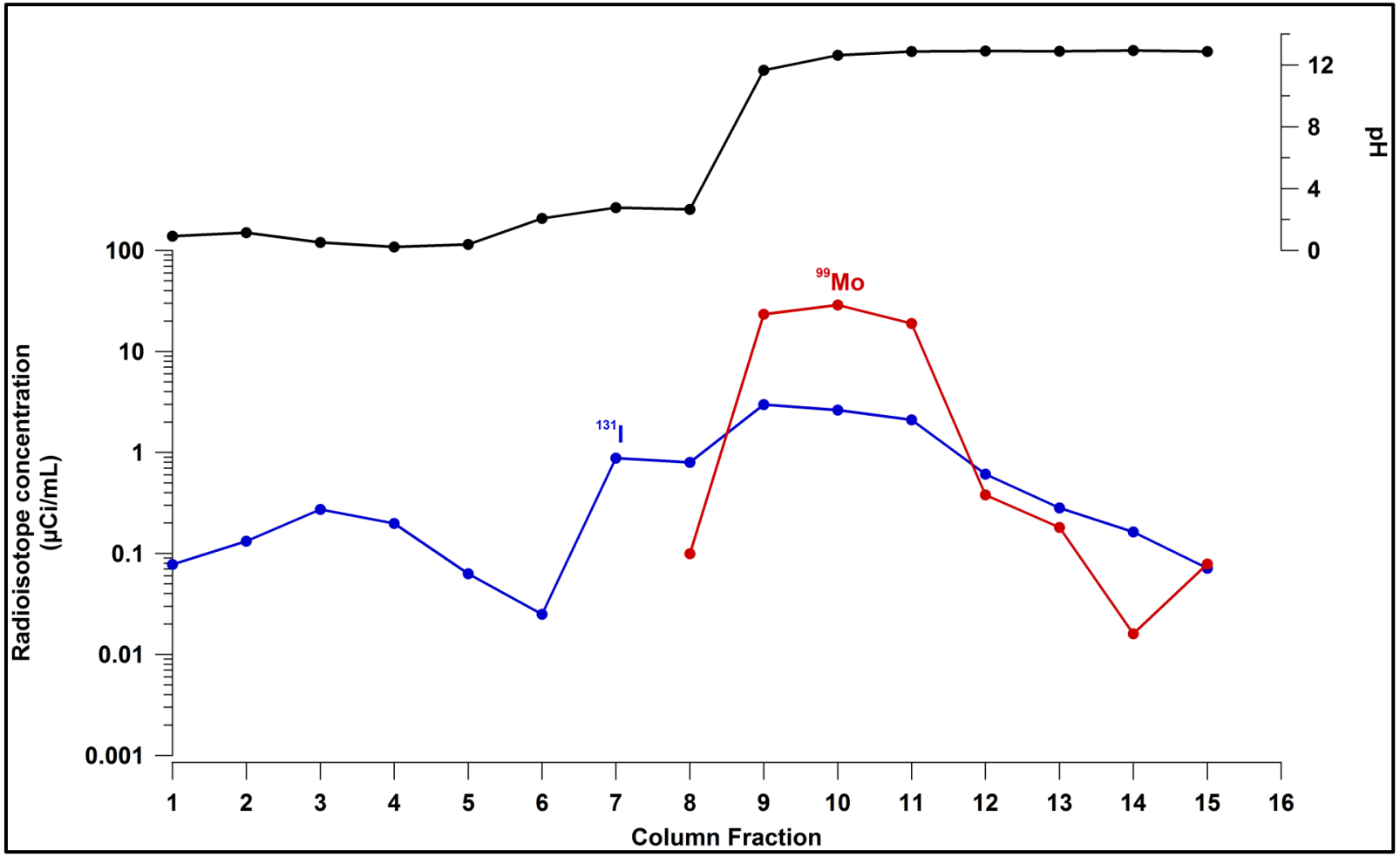

Figure 14. Third irradiation LEU sulfate solution column separation data for ^{131}I and ^{99}Mo. EOB for this irradiation was 28.0694. Radioisotope concentrations were calculated to end of column time, 31.9167.

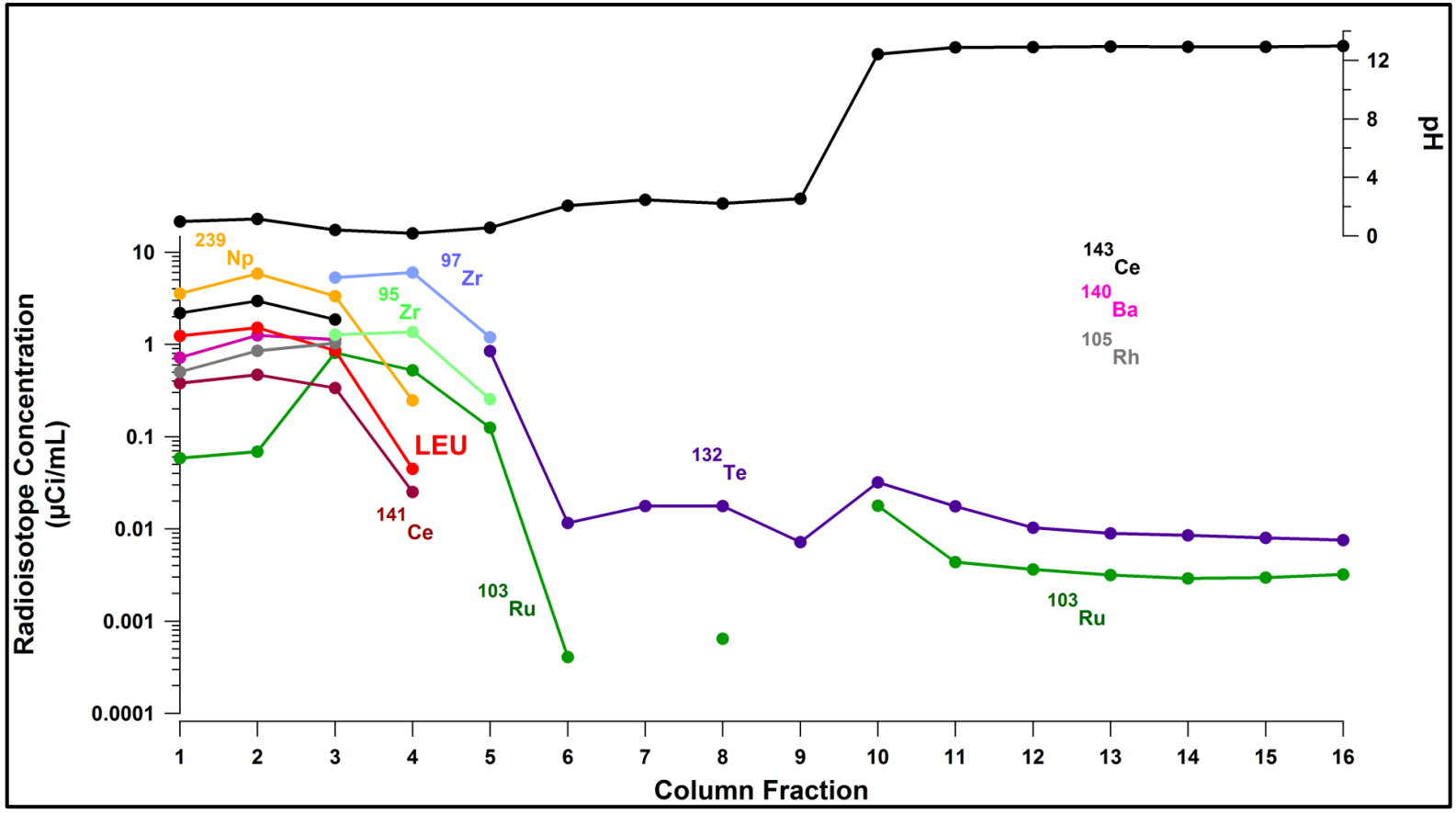

Figure 15. First irradiated LEU sulfate solution, column separation data for uranium (LEU), ^{239}Np, ^{103}Ru, ^{105}Rh, ^{141}Ce, ^{143}Ce, ^{140}Ba, ^{132}Te, ^{95}Zr and ^{97}Zr. EOB for this irradiation was 346.1326. Radioelement concentrations were calculated to end of column time, 349.0208.

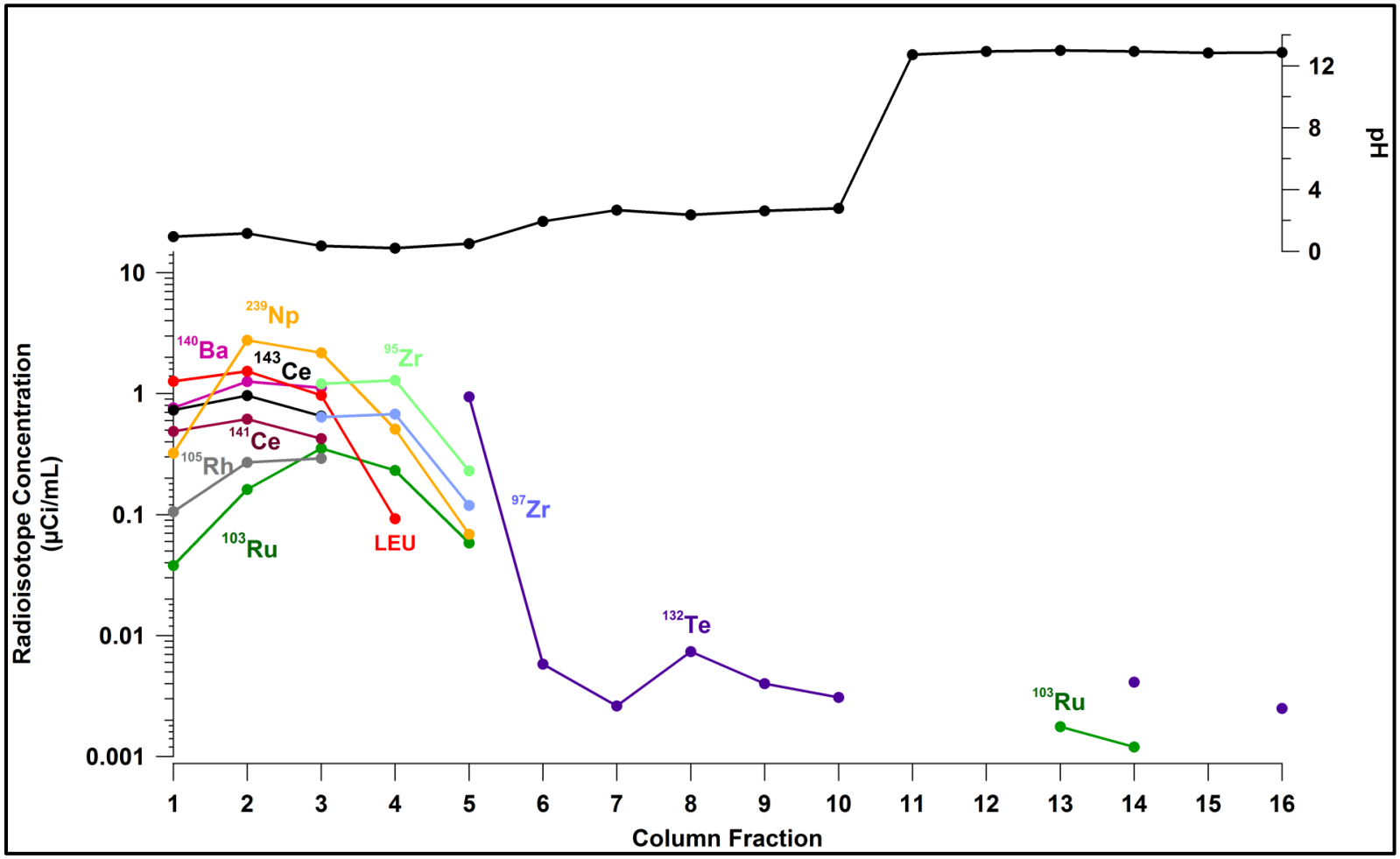

Figure 16. Second irradiation LEU sulfate solution, column separation data for uranium (LEU), ^{239}Np, ^{103}Ru, ^{105}Rh, ^{141}Ce, ^{143}Ce, ^{140}Ba, ^{132}Te, ^{95}Zr and ^{97}Zr. EOB for this irradiation was 9.9278. Radioelement concentrations were calculated to end of column time, 14.9076.

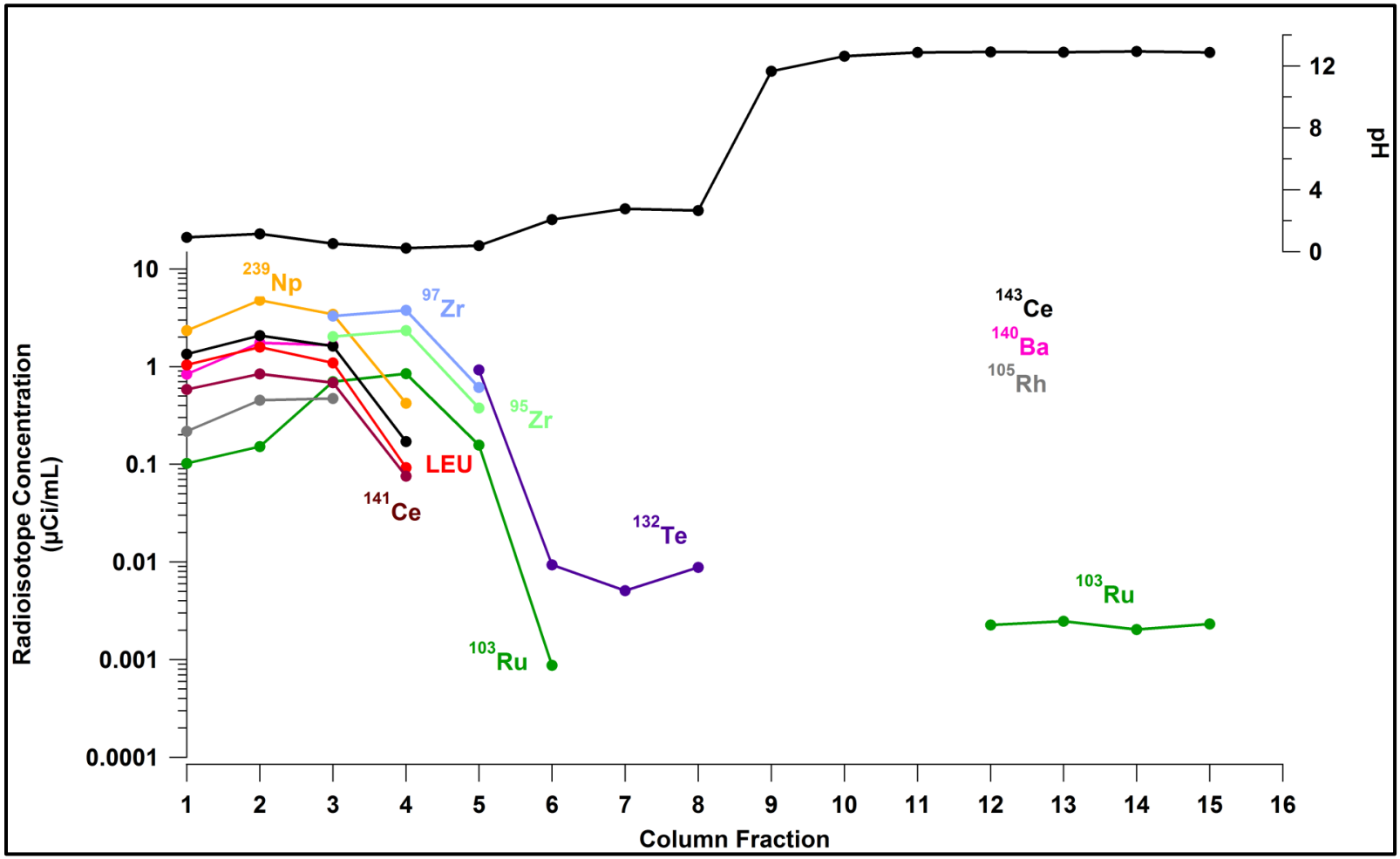

Figure 17. Third irradiated LEU sulfate solution, column separation data for uranium (LEU), ^{239}Np, ^{103}Ru, ^{105}Rh, ^{141}Ce, ^{143}Ce, ^{140}Ba, ^{132}Te, ^{95}Zr and ^{97}Zr. EOB for this irradiation was 28.0694. Radioelement concentrations were calculated to end of column time, 31.9167.

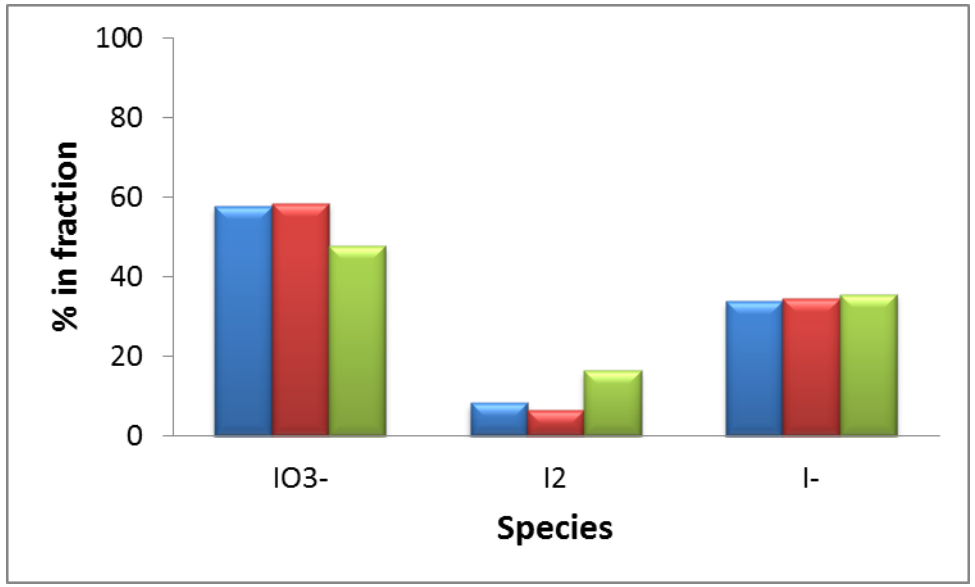

Figure 18. Iodine species in the 1st (blue), 2nd (red) and 3rd (green) irradiated LEU sulfate solutions. Percent in each fraction was calculated by dividing each fraction by the sum of all fractions.

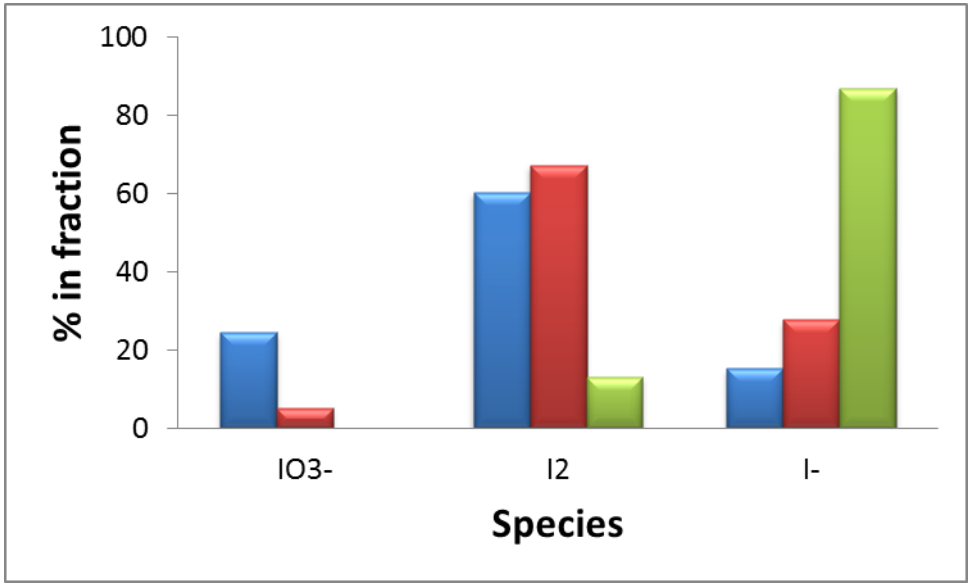

Figure 19. Iodine species from the 3rd irradiated LEU uranium sulfate solution column separation. Data for fractions 2 (blue, pH 1.15), 7 (red, pH 2.77) and 9 (green, pH 11.7) is presented. Percent in each fraction was calculated by dividing each fraction by the sum of all fractions.

Tables

Sample	Uranium concentration (g L^{-1})	Absorption at 420 nm	Epsilon calculated
1	2.243	0.129	13.69
2	3.743	0.215	13.67
3	5.248	0.301	13.65
4	6.744	0.387	13.66
5	8.253	0.473	13.64

Table 1. Experimental details for preparation of depleted uranyl sulfate standard solutions in 1 mol L^{-1} H_2SO_4, and the resultant visible spectroscopy absorption values used to calculate the molar absorptivity of the main uranyl band at λ_{max} 420 nm (ε = 13.65(±2) L mol^{-1} cm^{-1}).

	Sample	Uranium concentration (mol L^{-1})	Uranium concentration (g L^{-1})
1st pre-irradiation LEU sulfate solution	1	0.637	151
	2	0.634	150
	3	0.631	150
	Average	0.634(3)	150±1
2nd pre-irradiation LEU sulfate solution	1	0.644	153
	2	0.644	153
	3	0.647	154
	Average	0.645(2)	153±1
3rd pre-irradiation LEU sulfate solution	1	0.644	153
	2	0.641	152
	3	0.635	151
	Average	0.640(5)	152±1

Table 2. Uranium concentrations measured for the three LEU sulfate fuel solutions prior to the 1st, 2nd & 3rd irradiation, as determined using UV-vis spectrometry. The first pre-irradiation solution was the initially prepared LEU sulfate stock solution. Molar absorptivity and molecular weights used to calculate the uranium concentrations: ε = 13.65(±2) L mol^{-1} cm^{-1} and 237.41 g mol^{-1}, respectively. Nominal volumes (accurately determined) of 50 µL of sample and 2000 µL of 1 mol L^{-1} H_2SO_4 were used for the UV-vis assay.

	Sample	Uranium concentration (mol L^{-1})	Uranium concentration (g L^{-1})
1st post-irradiation LEU sulfate solution	1	0.653	155
	2	0.659	156
	3	0.662	157
	Average	0.658(5)	156±1
2nd post-irradiation LEU sulfate solution	1	0.638	151
	2	0.644	153
	3	0.644	153
	Average	0.642(3)	152±1
3rd Post-irradiation LEU sulfate solution		0.665	158

Table 3. Uranium concentration measurements for the three irradiated LEU sulfate solutions post-irradiation, as determined using UV-Vis spectrometry. The molar absorptivity and molecular weight used to calculate the uranium concentrations were ε = 13.65(±2) L mol^{-1} cm^{-1} and 237.41 g mol^{-1}, respectively. Nominal volumes (accurately determined) of 50 µL of sample and 2000 µL of 1 mol L^{-1} H_2SO_4 were used for UV-vis assay. The uranium concentration was only measured once for the 3rd irradiation.

Fraction	Sample description	Sample uranium concentration (mol L^{-1})	Uranium concentration (g L^{-1})
1	5 mL neat LEU solution	0.521	124
2	5 mL neat LEU bulk fraction	0.636	151
3	1 mol L^{-1} H_2SO_4 wash 1st 5 mL fxn	0.361	85.8
4	1 mol L^{-1} H_2SO_4 wash 2nd 5 mL fxn	0.189	4.48

Table 4. Uranium concentration measurements for column fractions 1 – 4 from the 1st irradiated LEU sulfate solution column separation, analyzed using UV-Vis spectrometry. The molar absorptivity and molecular weight used to calculate the uranium concentrations were ε = 13.65(±2) L mol^{-1} cm^{-1} and 237.41 g mol^{-1}, respectively. For fractions 1-3, nominal volumes (accurately determined) of 50 µL of sample and 2000 µL of 1 mol L^{-1} H_2SO_4 were used for UV-vis assay. Fraction 4 was taken to dryness and made up in a known volume of 1 mol L^{-1} H_2SO_4.

Fraction	Sample description	Sample uranium concentration (mol L^{-1})	Uranium Concentration (g L^{-1})
1	5 mL neat LEU	0.534	127
2	5 mL neat LEU bulk fraction	0.643	153
3	1 mol L^{-1} H_2SO_4 wash 1st 5 mL fxn	0.408	96.9
4	1 mol L^{-1} H_2SO_4 wash 2nd 5 mL fxn	0.039	9.24

Table 5. Uranium concentration measurements for column fractions 1 – 4 from the 2nd irradiated LEU sulfate solution column separation, analyzed using UV-Vis spectrometry. The molar absorptivity and molecular weight used to calculate the uranium concentrations were ε = 13.65(±2) L mol^{-1} cm^{-1} and 237.41 g mol^{-1}, respectively. For fractions 1-3, nominal volumes (accurately determined) of 50 µL of sample and 2000 µL of 1 mol L^{-1} H_2SO_4 were used for UV-vis assay. Fraction 4 was taken to dryness and made up in a known volume of 1 mol L^{-1} H_2SO_4.

Fraction	Sample description	Sample uranium concentration (mol L^{-1})	Uranium concentration (g L^{-1})
1	5 mL neat LEU	0.437	104
2	5 mL neat LEU bulk fraction	0.667	158
3	1 mol L^{-1} H_2SO_4 wash 1st 5 mL fxn	0.460	109
4	1 mol L^{-1} H_2SO_4 wash 2nd 5 mL fxn	0.039	9.24

Table 6. Uranium concentration measurements for column fractions 1 – 4 from the 3rd irradiated LEU sulfate solution column separation, analyzed using UV-Vis spectrometry. The molar absorptivity and molecular weight used to calculate the uranium concentrations were ε = 13.65(±2) L mol^{-1} cm^{-1} and 237.41 g mol^{-1}, respectively. For fractions 1-3, nominal volumes (accurately determined) of 50 µL of sample and 2000 µL of 1 mol L^{-1} H_2SO_4 were used for UV-vis assay. Fraction 4 was taken to dryness and made up in a known volume of 1 mol L^{-1} H_2SO_4.

	1st Irradiation	2nd Irradiation	3rd Irradiation
Irradiation date	11th Dec. '12	9th Jan. '13	28th Jan. '13
Solution density pre-irradiation (g mL^{-1})	1.193(1)	1.203(3)	1.208(3)
Solution density post-irradiation (g mL^{-1})	1.198(2)	1.203(4)	1.206(1)
Mass of LEU sulfate (g)	178.76	180.13	180.14
Volume of LEU sulfate (mL)	150.30	150.10	148.88
Volume of 10.08 mmol L^{-1} Na_2MoO_4 (aq, µL)	53.0	52.7	52.6
Mo conc. (mmol L^{-1}) in final LEU soln.	3.55×10^{-3}	3.54×10^{-3}	3.56×10^{-3}
pH before irradiation	1.0	1.2	1.1
pH after irradiation	1.1	1.2	1.2
% recycle irradiated uranium	0 %	78 %	77 %
End of beam time (EOB)	346.1326	9.9278	28.0694

Table 7. Experimental details for the three irradiated LEU sulfate solutions.

Step	Media	Flow rate (mL min^{-1})	Flow direction	Solution volume (mL)
Pre-equilibrium	0.1 mol L^{-1} H_2SO_4	2.83	Up	< 20
Load	Irradiated LEU sulfate solution	1.07	Up	128 – 136
Wash	1 mol L^{-1} H_2SO_4	2.83	Up	11.31
Wash	H_2O	2.83	Up	20
Strip	0.1 mol L^{-1} NaOH	1.41	Down	40

Table 8. Solution feed operating parameters for the downscale column separation processes.

Sample description	Gold mass (mg)	^{198}Au (412 KeV) dpm	µCi	µCi mg^{-1} Au
Gold foil	16.8	26710000(0.6)	12.03(0.07)	0.716
Gold foil inside Cd envelope	17.2	9692000(0.7)	4.37(0.03)	0.254

Table 9. Gamma spectrometry results back calculated to EOB for the gold foils (encapsulated and not encapsulated in Cd) irradiated during the water irradiation experiment. (dpm = disintegrations per minute).

	Water	H_2SO_4	1st irradiation	2nd irradiation	3rd irradiation
Collected gas pressure (Torr)	-8.63	452	284	292	409
Collected gas pressure (µmoles)	-28.3	1484	932	959	1342

Table 10. Collected gas pressure data obtained from the irradiated water, irradiated 0.1 mol L^{-1} H_2SO_4 and three irradiate LEU sulfate samples. Boyle's Law ($P_1V_1 = P_2V_2$; where P_1 = pressure of gas generated, V_1 = 60 cc headspace of inner container, P_2 = pressure of gas recorded after gas generated expansion, V_2 = expansion volume of 575 cc: 500 cc cylinder + 60 cc headspace + 15 cc manifold volume) was applied to determine the gas pressure generated during irradiation (collected gas pressure). Collected gas pressures in µmoles were determine using the Ideal Gas Law (PV = nRT).

Sample	% H_2*	% O_2*	H_2/O_2
Water	ND	ND	NA
0.1 mol L^{-1} H_2SO_4	36.0	ND	NA
1st Irradiation	27.9	7.6	3.7
2nd Irradiation	26.2	5.6	4.6
3rd Irradiation	26.0	6.5	4.0
4 % H_2/Ar calibration mixture	4.0	ND	NA
6 % O_2/Ar calibration mixture	ND	6.0	NA

Table 11. Gas composition from mass spectrometry analysis of collected gas samples from the irradiated water sample, the irradiated 0.1 mol L^{-1} H_2SO_4 sample and the three LEU sulfate solutions. * % H_2 and O_2 values are corrected by multiplying the pressures obtained by their correction factors, 0.46 and 2.0, respectively. Correction factors were calculated as follow: in a standard 4 % H_2/Ar mixture, the RGA found an H_2 percentage of 8.7 % (taken by dividing the partial pressure of H_2 by the sum of the partial pressures), while in a 6 % O_2/Ar mixture the oxygen pressure detected by the RGA was 3 %. By dividing 4 % (expected) H_2/Ar mixture by 8.7 % (observed) a correction factor of 0.46 for hydrogen was obtained. The correction factor for oxygen was calculated similarly. ND = none detected, NA = not applicable.

Sample	Cr (µg)	Ni (µg)	Mn (µg)	Fe (µg)
FT1	30(2)	13(1)	2.0(1)	122(7)
FT2	30(2)	13(1)	2.0(2)	127(7)
FT3	31(3)	13(1)	2.0(1)	125(6)
FT4	33(1)	13(1)	2.0(1)	130(8)
FT5	32(3)	14(1)	2.0(1)	132(7)
FT6	33(2)	15(1)	2(0.1)	133(11)
FT7	33(2)	14(1)	2.0(2)	127(8)
FT8	35(2)	15(1)	2.0(2)	131(7)
Average (STD) (FT1 – FT8)	32(2)	14(1)	2(1)	128(4)
Concentration (mg L^{-1})	325	143	25	1288
Concentration (mg) in 150 mL sample	48	21	3	192

Table 12. ICP-MS results on the 150 mL irradiated 0.1 mol L^{-1} H_2SO_4 solution post-irradiation. Eight samples were collected (FT1 through FT8) and each sample was composed of 100 µL of solution. Numbers in parenthesis are uncertainties.

Irradiated Sample	Sample volume measured/total (mL)	Measured time	dpm at EOB (% error)	µCi in measured sample	µCi total sample	µCi Average(STD)
1st Irradiation	1.24/149.3	353.9766	19560000(0.9)	9	1064	1044(17)
1st Irradiation	1.24/149.3	354.0503	19090000(0.6)	9	1037	
1st Irradiation	1.24/149.3	354.1700	18950000(0.9)	9	1031	
2nd Irradiation	4.96/145.3	15.3661	66390000(1.6)	30	876	876(23)
2nd Irradiation	1.23/145.3	16.9146	17010000(1.3)	8	906	
2nd Irradiation	1.23/145.3	17.0624	16400000(1.3)	7	872	
2nd Irradiation	1.23/145.3	17.1371	16030000(1.3)	7	850	
3rd Irradiation	4.97/149.3	35.9478	77050000(1.7)	35	1043	1063(57)
3rd Irradiation	1.23/149.3	36.1125	18590000(1.4)	8	1016	
3rd Irradiation	1.23/149.3	36.2309	20990000(1.5)	9	1146	
3rd Irradiation	1.23/149.3	36.3050	19220000(1.5)	9	1149	

Table 13. ^{99}Mo Production values for the 181 KeV transitions in the three irradiated LEU sulfate solutions (dpm = disintegrations per minute). Data corrected to EOB.

Irradiated Sample	Sample volume measured/total (mL)	Measured time	dpm at EOB (% error)	µCi in measured sample	µCi total sample	µCi Average(STD)
1st Irradiation	1.24/149.3	354.0503	19030000(1.3)	9	1033	1000(30)
1st Irradiation	1.24/149.3	355.9859	18130000(1.0)	8	986	
1st Irradiation	1.24/149.3	356.0590	17990000(1.0)	8	978	
2nd Irradiation	4.96/145.3	16.9889	65210000(1.5)	29	861	886(20)
2nd Irradiation	1.23/145.3	16.9146	17060000(1.4)	8	909	
2nd Irradiation	1.23/145.3	17.1371	16860000(1.5)	8	894	
2nd Irradiation	1.23/145.3	17.0624	16550000(1.4)	7	880	
3rd Irradiation	4.97/149.3	35.9478	81620000(1.7)	37	1105	1087(22)
3rd Irradiation	1.23/149.3	36.1125	19630000(1.4)	9	1073	
3rd Irradiation	1.23/149.3	36.2309	20290000(1.5)	9	1107	
3rd Irradiation	1.23/149.3	36.305	19490000(1.5)	9	1063	

Table 14. ^{99}Mo Production values for the 740 KeV transitions in the three irradiated LEU sulfate solutions (dpm = disintegrations per minute). Data corrected to EOB.

Irradiated sample	Sample volume measured/total (mL)	Measured time	dpm at EOB (% error)	µCi at EOB	µCi after 72 Hours	72 hours µCi Average(STD)
1st Irradiation	1.24/149.3	353.9766	2890000(0.6)	157	121	121(1)
1st Irradiation	1.24/149.3	356.0590	2914000(0.6)	158	122	
1st Irradiation	1.24/149.3	354.0503	2909000(0.6)	158	122	
2nd Irradiation	4.96/145.3	15.3661	10640000(0.7)	140	108	108(1)
2nd Irradiation	1.23/145.3	24.6790	2638000(0.6)	140	107	
2nd Irradiation	1.23/145.3	24.0074	2637000(0.6)	140	108	
2nd Irradiation	1.23/145.3	23.8625	2650000(0.6)	141	108	
3rd Irradiation	4.97/149.3	35.9478	12970000(0.6)	175	135	135(1)
3rd Irradiation	1.23/149.3	36.1125	3210000(0.6)	175	135	
3rd Irradiation	1.23/149.3	36.2309	3177000(0.6)	173	133	
3rd Irradiation	1.23/149.3	36.3050	3183000(0.6)	173	134	

Table 15. ^{131}I (365 KeV) Production values for the three irradiated LEU sulfate solutions (dpm = disintegrations per minute). Data corrected to 72 hours after EOB in each case to account for ingrowth of ^{131}I from ^{131}Te and ^{131m}Te. The amount ^{131}I present in the irradiated fuel after the 2nd and 3rd irradiations attributed to recycled material from the 1st and 2nd irradiations was calculated to be 0.42 and 1.30 µCi, respectively. As this accounts for less than 1 % of the total ^{131}I present in both the 2nd and 3rd irradiated fuels then they have no significant contribution to the 2nd and 3rd irradiation production values.

Irradiated sample	Sample volume measured/total (mL)	Measured time	dpm at EOB (% error)	µCi at EOB	µCi Average(STD)
1st Irradiation	4.96/149.3	353.927	144100000(0.6)	1953	2033(56)
1st Irradiation	1.24/149.3	353.9766	38160000(0.6)	2076	
1st Irradiation	1.24/149.3	354.0503	38030000(0.6)	2065	
1st Irradiation	1.24/149.3	354.0503	37400000(0.6)	2034	
2nd Irradiation	4.96/145.3	15.3661	131900000(0.7)	1741	1695(35)
2nd Irradiation	1.23/145.3	16.9146	31580000(0.8)	1682	
2nd Irradiation	1.23/145.3	17.1371	32030000(0.8)	1699	
2nd Irradiation	1.23/145.3	17.0624	31170000(0.8)	1657	
3rd Irradiation	4.97/149.3	35.9478	162000000(0.8)	2193	2167(26)
3rd Irradiation	1.23/149.3	36.1125	39860000(0.7)	2179	
3rd Irradiation	1.23/149.3	36.2309	39080000(0.7)	2133	
3rd Irradiation	1.23/149.3	36.3050	39640000(0.7)	2164	

Table 16. ^{239}Np (278 KeV) production values for the three irradiated LEU sulfate solutions (dpm = disintegrations per minute). Data corrected to EOB. The recycle ^{239}Np activities carried over to the 2nd and 3rd irradiations were very low (2nd = 0.237 µCi; 3rd = 0.314 µCi) and did not impact the analysis.

Irradiated sample	Sample volume measured/total (mL)	Measured time	dpm at EOB (% error)	µCi at EOB	µCi average(STD)
1st Irradiation	4.96/149.3	353.927	141000000(0.6)	1911	1976(53)
1st Irradiation	1.24/149.3	353.9766	36510000(0.9)	1986	
1st Irradiation	1.24/149.3	354.0503	37600000(0.6)	2042	
1st Irradiation	1.24/149.3	354.17	36100000(0.9)	1964	
2nd Irradiation	4.96/145.3	14.6476	131600000(0.9)	1737	1756(58)
2nd Irradiation	1.23/145.3	12.0588	34300000(0.9)	1819	
2nd Irradiation	1.23/145.3	12.0356	33530000(0.9)	1783	
2nd Irradiation	1.23/145.3	16.9146	31640000(0.9)	1685	
3rd Irradiation	4.97/149.3	35.9478	164000000(1.2)	2220	2109(76)
3rd Irradiation	1.23/149.3	36.1125	38430000(1.1)	2101	
3rd Irradiation	1.23/149.3	36.2309	37600000(1.2)	2052	
3rd Irradiation	1.23/149.3	36.305	37830000(1.2)	2065	

Table 17. ^{143}Ce (293 KeV) Production values for the three irradiated LEU sulfate solutions (dpm = disintegrations per minute). Data corrected to EOB. The recycled ^{143}Ce carried over to the 2nd and 3rd irradiations was minimum (2nd = 0.0004 µCi; 3rd = 0.1471 µCi at EOB) and did not impact the analysis.

Irradiated sample	Sample volume measured/total (mL)	Measured time	dpm at EOB (% error)	µCi at EOB	µCi average(STD)
1st Irradiation	1.24/149.3	353.9766	1562000(0.6)	85	85.5(1)
1st Irradiation	1.24/149.3	354.0503	1573000(0.6)	86	
1st Irradiation	1.24/149.3	354.1700	1558000(0.6)	85	
2nd Irradiation	1.23/145.3	17.1371	2037000(0.6)	108	107(1) 77*
2nd Irradiation	1.23/145.3	17.0624	2006000(0.6)	107	
2nd Irradiation	1.23/145.3	16.9146	2009000(0.6)	107	
3rd Irradiation	1.23/149.3	36.1125	2738000(0.6)	150	143(1) 93*
3rd Irradiation	1.23/149.3	36.2309	2726000(0.6)	149	
3rd Irradiation	1.23/149.3	36.3050	2749000(0.6)	150	

Table 18. ^{141}Ce (145 KeV) production values for the three irradiated LEU sulfate solutions (dpm = disintegrations per minute). Data corrected to EOB. *These values were obtained by subtracting the ^{141}Ce introduced with the recycled fuel, again corrected to EOB, (2nd = 30 µCi; 3rd = 50 µCi) from the total average value. Only diluted samples (*c.a.* 1.25 mL + 3.75 mL H_2SO_4) were used, the neat samples yielded activities values that were systematically 10% lower.

Irradiated sample	Sample volume measured/total (mL)	Measured time	dpm at EOB (% error)	µCi after 24 hours	24 hours µCi average(STD)
1st Irradiation	1.24/149.3	356.059	848200(1.0)	45.9	46.2(0.3)
1st Irradiation	1.24/149.3	356.6715	856200(1.0)	46.2	
1st Irradiation	1.24/149.3	356.8872	859800(1.0)	46.5	
2nd Irradiation	1.23/145.3	24.6790	834900(0.9)	41.6	41.6(0.4)
2nd Irradiation	1.23/145.3	24.0074	826200(0.9)	41.2	
2nd Irradiation	1.23/145.3	23.8625	840400(0.9)	42.0	
3rd Irradiation	1.23/149.3	36.1125	946200(1.2)	51.2	51.9(0.5)
3rd Irradiation	1.23/149.3	36.2309	962200(1.1)	52.0	
3rd Irradiation	1.23/149.3	36.3050	960300(1.1)	51.8	

Table 19. ^{95}Zr (743 KeV) production values for the three irradiated LEU sulfate solutions (dpm = disintegrations per minute). Data corrected to 24 hours after EOB.

Irradiated sample	Sample volume measured/total (mL)	Measured time	dpm at EOB (% error)	µCi at EOB	µCi Average(STD)
1st Irradiation	4.96/149.3	353.9270	17970000	243	228(10)
1st Irradiation	1.24/149.3	355.9859	4177000(0.8)	227	
1st Irradiation	1.24/149.3	356.6715	4098000(0.8)	222	
1st Irradiation	1.24/149.3	356.8872	4070000(0.8)	221	
2nd Irradiation	4.96/145.3	24.9151	17940000(1.1)	237	237(6) 202*
2nd Irradiation	1.23/145.3	17.1371	4437000(0.8)	235	
2nd Irradiation	1.23/145.3	17.0624	4328000(0.8)	230	
2nd Irradiation	1.23/145.3	23.8625	4585000(0.6)	244	
3rd Irradiation	4.97/149.3	35.9478	23690000(0.8)	321	318(8) 250*
3rd Irradiation	1.23/149.3	36.1125	5755000(0.8)	315	
3rd Irradiation	1.23/149.3	36.2309	5983000(0.8)	327	
3rd Irradiation	1.23/149.3	36.3050	5648000(0.8)	308	

Table 20. ^{140}Ba (537 KeV) production values for the three irradiated LEU sulfate solutions (dpm = disintegrations per minute). Data corrected to EOB. *These activities were obtained by subtracting the ^{140}Ba introduced with the recycled fuel (2nd = 35 µCi; 3rd = 68 µCi) from the total average activities, with again activities corrected to EOB.

Irradiated sample	Sample volume measured/total (mL)	Measured time	dpm at EOB (% error)	µCi after 72 hours	72 hours µCi average(STD)
1st Irradiation	1.24/149.3	353.9766	1950000(0.7)	88.2	88.8(1.4)
1st Irradiation	1.24/149.3	356.0590	2010000(0.6)	90.9	
1st Irradiation	1.24/149.3	356.6715	1934000(0.6)	87.3	
2nd Irradiation	1.23/145.3	24.6790	2310000(0.7)	101	97.5(5.7) 88.2*
2nd Irradiation	1.23/145.3	24.0074	2280000(0.7)	100	
2nd Irradiation	1.23/145.3	23.8625	2063000(0.7)	90.9	
3rd Irradiation	1.23/149.3	36.1125	3070000(2.1)	139	134(5) 114*
3rd Irradiation	1.23/149.3	36.2309	2945000(2.1)	133	
3rd Irradiation	1.23/149.3	36.3050	3017000(6.3)	136	

Table 21. ^{147}Nd (91 KeV) Production values for the three irradiated LEU sulfate solutions (dpm = disintegrations per minute). Data corrected to 72 hours after EOB. *These values were obtained by subtracting the ^{147}Nd introduced with the recycled fuel (2nd = 9.3 µCi; 3rd = 20.3 µCi, corrected to 72 hours after EOB) from the total average value.

Irradiated sample	Sample volume measured/total (mL)	Measured time	dpm at EOB (% error)	µCi at EOB	µCi Average(STD)
1st Irradiation	4.96/149.3	353.9270	2651000(0.9)	35.9	35.6(0.4)
1st Irradiation	1.24/149.3	355.9859	648600(0.7)	35.3	
1st Irradiation	1.24/149.3	356.6715	661100(0.7)	35.9	
1st Irradiation	1.24/149.3	356.8872	648200(0.7)	35.3	
2nd Irradiation	4.96/145.3	24.9151	2853000(0.9)	37.7	38.4(0.5) 33.7*
2nd Irradiation	1.23/145.3	24.6790	730400(0.7)	38.7	
2nd Irradiation	1.23/145.3	24.0074	727800(0.7)	38.7	
2nd Irradiation	1.23/145.3	23.8625	726900(0.7)	38.7	
3rd Irradiation	4.97/149.3	35.9478	4071000(0.9)	55.1	54.5(0.5) 40.1*
3rd Irradiation	1.23/149.3	36.1125	986300(0.9)	53.9	
3rd Irradiation	1.23/149.3	36.2309	995900(0.9)	54.4	
3rd Irradiation	1.23/149.3	36.3050	1004000(0.9)	54.8	

Table 22. ^{103}Ru (497 KeV) production values for the three irradiated LEU sulfate solutions (dpm = disintegrations per minute). Data corrected to EOB. *These values were obtained by subtracting the ^{103}Ru introduced with the recycled fuel (2nd = 4.7(1) µCi; 3rd = 14.4 µCi at EOB) from the total average value.

	Irradiated solution pre-contact (µCi)	Irradiated solution post-contact Both activity in µCi and % in Fraction			0.1 mol L^{-1} NaOH solution post-contact Both activity in µCi and % in fraction			Irreversibly bound to TiO_2 (µCi)	Activity balance (%)		
	1.25 mL Sample	Sample 1 pH 1.10	Sample 2 pH 1.11	Sample 3 pH 1.16	Sample 1 pH 12.87	Sample 2 pH 12.85	Sample 3 pH 12.91	Sample 3 (µCi), %	Sample 1	Sample 2	Sample 3
^{239}Np (278 keV)	7.276 (0.6)	7.204(0.6) 99	7.210(0.6) 99	7.253(0.6) 100	NDA	NDA	NDA	NDA	99	99	100
^{141}Ce (145 keV)	0.674(0.5)	0.684(0.7) 101	0.700(0.7) 104	0.683(0.7) 101	NDA	NDA	NDA	NDA	101	104	101
^{143}Ce (239 keV)	3.864(0.5)	3.796(0.6) 98	3.786(0.6) 98	3.816(0.6) 99	NDA	NDA	NDA	NDA	98	98	99
^{140}Ba (537 keV)	1.601 (0.8)	1.587(1.1) 99	1.561(1.1) 98	1.559(1.1) 97	NDA	NDA	NDA	NDA	99	98	97
^{95}Zr (319 keV)	0.380(1.0)	0.023(12) 6	0.018(14) 5	0.013(22) 3	NDA	NDA	NDA	0.329(1.2) 87	6*	5*	90
^{97}Zr (743 keV)	1.691(0.7)	0.091(3.1) 5	0.062(4) 4	0.066(3.5) 4	NDA	NDA	NDA	1.358(3.3) 80	5*	4*	84
^{103}Ru (497 keV)	0.283(0.8)	0.119(2.4) 42	0.115(2.4) 40	0.119(1.4) 42	0.016(4.1) 6	0.015(3.8) 5	0.016(3.4) 6	0.137(1.3) 48	48*	45*	96
^{131}I (365 keV)	1.022(0.6	0.267(6.7) 26	0.247(9) 24	0.265(7.5) 26	0.486(0.9) 48	0.523(0.8) 51	0.475(0.9) 46	0.127(1.2) 13	74*	75*	85
^{99}Mo (181 keV)	4.168(0.9)	0.370(6.6) 9	NDA	0.254(7.8) 6	3.731(0.6) 88	4.191(0.6) 99	3.998(0.6) 94	NDA	97	99	100
^{99}Mo (740 keV)	4.048(1.0)	0.261(6.7) 6	0.154(9) 4	0.176(7.5) 4	3.604(0.9) 89	4.038(0.8) 99	3.843(0.9) 95	NDA	95	103	99

Table 23. Batch separation data obtained from samples of the 1st irradiated LEU sulfate solution. Radioisotope concentrations were calculated to end of column time for the 1st column separation experiment, 349.0208. EOB for this irradiation was 346.1326. *From analysis of TiO_2 in sample 3 it can be assumed that the poorer activity balances reported for these radioisotopes is due to a fraction of that isotope binding to TiO_2. Numbers in parenthesis are % errors.

Radioisotope	K_d (mL g^{-1}) in irradiated soln. post-contact		
	Sample 1	Sample 2	Sample 3
^{97}Zr	1420	2249	2064
^{95}Zr	1249	1708	2365
^{103}Ru	111	125	115
^{99}Mo	825	>1289	1289

Table 24. ^{97}Zr, ^{103}Ru and ^{99}Mo Distribution coefficient (K_d) values for the TiO_2 batch contact experiments with the 1st irradiated LEU sulfate solution.

	Fxn 1	Fxn 2	Fxn 3	Fxn 4	Fxn 5	Fxn 6	Fxn 7	Fxn 8	Fxn 9	Fxn 10	Fxn 11	Fxn 12	Fxn 13	Fxn 14	Fxn 15	Fxn 16	Irreversibly bound to TiO_2 (µCi)	Activity balance (%)
pH	0.99	1.15	0.41	0.18	0.55	2.06	2.47	2.22	2.54	12.42	12.88	12.90	12.94	12.92	12.93	12.97	NDA	NDA
Volume	5.11	120.6	4.90	4.69	9.79	10.1	7.61	7.56	4.92	4.39	4.93	5.10	4.97	4.83	5.09	5.05	NDA	NDA
Uranium	1.24	1.51	0.86	0.04	NDA	NDA	NDA	NDA	NDA	NDA	NDA	NDA	NDA	NDA	NDA	NDA	NDA	96
^{239}Np 278 keV	3.55 (0.6)	5.83 (0.8)	3.33 (1.5)	0.25 (6.9)	NDA	NDA	NDA	NDA	NDA	NDA	NDA	NDA	NDA	NDA	NDA	NDA	NDA	98
^{141}Ce 145 keV	0.38 (0.6)	0.47 (0.7)	0.34 (1.2)	0.02 (6.9)	NDA	NDA	NDA	NDA	NDA	NDA	NDA	NDA	NDA	NDA	NDA	NDA	NDA	96
^{143}Ce 239 keV	2.19 (0.8)	2.95 (1.2)	1.86 (2.1)	NDA	NDA	NDA	NDA	NDA	NDA	NDA	NDA	NDA	NDA	NDA	NDA	NDA	NDA	94
^{140}Ba 537 keV	0.72 (1.1)	1.25 (0.8)	1.13 (2.5)	NDA	NDA	NDA	NDA	NDA	NDA	NDA	NDA	NDA	NDA	NDA	NDA	NDA	NDA	97
^{105}Rh 319 keV	0.50 (2.8)	0.85 (5.0)	1.03 (9.8)	NDA	NDA	NDA	NDA	NDA	NDA	NDA	NDA	NDA	NDA	NDA	NDA	NDA	NDA	153*
^{95}Zr 757 keV	NDA	NDA	1.27 (1.4)	1.37 (0.8)	0.25 (1.0)	NDA	NDA	NDA	NDA	NDA	NDA	NDA	NDA	NDA	NDA	NDA	23(0.7)	101
^{97}Zr 743 keV	NDA	NDA	5.31 (3.5)	6.01 (1.7)	1.19 (4.2)	NDA	NDA	NDA	NDA	NDA	NDA	NDA	NDA	NDA	NDA	NDA	94(0.7)	91
^{103}Ru 497 keV	0.06 (1.5)	0.07 (3.8)	0.81 (0.9)	0.52 (0.7)	0.12 (1.0)	$4e^{-4}$ (11)	NDA	6e-4 (9.0)	NDA	0.02 (8.9)	$4e^{-3}$ (1.4)	$4e^{-3}$ (2.8)	$3e^{-3}$ (2.6)	$3e^{-3}$ (2.6)	$3e^{-3}$ (2.0)	$3e^{-3}$ (2.0)	12(0.7)	96
^{132}Te 228 keV	NDA	NDA	NDA	NDA	0.85 (1.0)	0.01 (1.7)	0.01 (2.9)	0.01 (2.9)	$7e^{-3}$ (5.6)	0.03 (18)	0.02 (15)	0.01 (2.0)	$8e^{-3}$ (1.8)	$8e^{-3}$ (1.6)	$8e^{-3}$ (1.3)	$7e^{-3}$ (1.3)	176(0.5)	67
^{131}I 365 keV	NDA	0.06 (3.7)	0.28 (2.1)	0.13 (1.6)	0.05 (1.5)	0.03 (1.2)	3.44 (0.5)	0.42 (0.7)	0.31 (0.8)	5.46 (0.6)	2.71 (0.7)	0.74 (0.5)	0.26 (0.6)	0.12 (0.6)	0.08 (0.6)	0.06 (0.7)	4(1.4)	85
^{99}Mo 181 keV	NDA	NDA	NDA	NDA	NDA	NDA	NDA	NDA	0.07 (9.3)	75.5 (0.5)	16.4 (0.6)	0.42 (1.0)	0.17 (1.6)	0.10 (2.3)	0.08 (2.1)	0.07 (2.1)	NDA	96
^{99}Mo 740 keV	NDA	NDA	NDA	NDA	NDA	NDA	NDA	NDA	0.07 (8.1)	73.5 (0.8)	15.8 (1.3)	0.42 (1.3)	0.17 (1.9)	0.10 (2.8)	0.08 (2.3)	0.06 (2.7)	NDA	97

Table 25. Column separation data for the 1st irradiated LEU sulfate solution. Radioisotope concentrations (µCi mL^{-1}) were calculated from gamma spectroscopy to end of column time, 349.0208, except for uranium concentrations which were measured by UV-vis spectroscopy as mol L^{-1} and subsequently converted to uCi mL^{-1}. EOB for this irradiation was 346.1326. ^{131}I concentration for the first fraction had a large count error and it was not included in this table. Numbers in parenthesis are % errors. *^{105}Rh has poor activity balance.

	Fxn 1	Fxn 2	Fxn 3	Fxn 4	Fxn 5	Fxn 6	Fxn 7	Fxn 8	Fxn 9	Fxn 10	Fxn 11	Fxn 12	Fxn 13	Fxn 14	Fxn 15	Fxn 16	Irreversibly bound to TiO_2 (µCi)	Activity balance (%)
pH	0.96	1.17	0.36	0.21	0.50	1.94	2.67	2.37	2.63	2.79	12.72	12.93	12.99	12.93	12.84	12.87	NDA	NDA
Volume	4.99	118.7	5.18	5.01	10.1	10.1	7.50	7.30	2.35	2.41	4.84	4.87	4.88	5.22	4.78	9.61	NDA	NDA
Uranium	1.27	1.53	0.97	0.09	NDA	NDA	NDA	NDA	NDA	NDA	NDA	NDA	NDA	NDA	NDA	NDA	NDA	99
^{239}Np 278 keV	0.32 (1.5)	2.80 (0.9)	2.18 (1.1)	0.51 (4.4)	0.07 (4.2)	NDA	NDA	NDA	NDA	NDA	NDA	NDA	NDA	NDA	NDA	NDA	NDA	100
^{141}Ce 145 keV	0.49 (0.6)	0.62 (0.8)	0.43 (1.3)	NDA	NDA	NDA	NDA	NDA	NDA	NDA	NDA	NDA	NDA	NDA	NDA	NDA	NDA	102
^{143}Ce 239 keV	0.73 (0.7)	0.97 (0.9)	0.65 (1.6)	NDA	NDA	NDA	NDA	NDA	NDA	NDA	NDA	NDA	NDA	NDA	NDA	NDA	NDA	98
^{140}Ba 537 keV	0.76 (0.9)	1.26 (1.0)	1.12 (1.7)	NDA	NDA	NDA	NDA	NDA	NDA	NDA	NDA	NDA	NDA	NDA	NDA	NDA	NDA	100
^{105}Rh 319 keV	0.11 (3.1)	0.27 (3.6)	0.29 (7.2)	NDA	NDA	NDA	NDA	NDA	NDA	NDA	NDA	NDA	NDA	NDA	NDA	NDA	NDA	226*
^{95}Zr 757 keV	NDA	NDA	1.20 (1.1)	1.29 (1.2)	0.23 (1.0)	NDA	NDA	NDA	NDA	NDA	NDA	NDA	NDA	NDA	NDA	NDA	20(1.3)	99
^{97}Zr 743 keV	NDA	NDA	5.31 (3.5)	6.01 (1.7)	1.19 (4.2)	NDA	NDA	NDA	NDA	NDA	NDA	NDA	NDA	NDA	NDA	NDA	10(2.0)	100
^{103}Ru 497 keV	0.04 (2.0)	0.16 (1.6)	0.35 (1.4)	0.23 (2.0)	0.06 (1.5)	NDA	NDA	NDA	NDA	NDA	NDA	NDA	$2e^{-3}$ (4.8)	$1e^{-3}$ (3.4)	NDA	NDA	7(0.7)	99
^{132}Te 228 keV	NDA	NDA	NDA	NDA	0.94 (0.6)	$6e^{-3}$ (1.3)	$3e^{-3}$ (17)	$7e^{-3}$ (2.9)	$4e^{-3}$ (6.9)	$3e^{-3}$ (11)	NDA	NDA	$5e^{-3}$ (2.2)	$4e^{-3}$ (1.3)	NDA	$2e^{-3}$ (1.2)	69(1.0)	55
^{131}I 365 keV	0.06 (1.2)	0.10 (2.1)	0.10 (3.5)	0.26 (1.6)	0.28 (0.6)	0.04 (1.3)	1.07 (0.6)	0.17 (0.8)	0.20 (1.1)	0.40 (0.6)	1.60 (1.0)	2.0 (0.8)	0.40 (0.5)	0.18 (0.6)	$2e^{-3}$ (1.6)	0.04 (0.6)	2(4.1)	81
^{99}Mo 181 keV	NDA	NDA	NDA	NDA	NDA	NDA	NDA	NDA	NDA	2.31 (0.7)	29.0 (0.6)	17.4 (0.7)	0.24 (0.7)	0.08 (1.2)	0.004 (2.3)	0.009 (2.1)	NDA	107
^{99}Mo 740 keV	NDA	NDA	NDA	NDA	NDA	NDA	NDA	NDA	NDA	2.24 (0.7)	28.2 (0.6)	16.8 (0.7)	0.24 (0.9)	0.08 (1.2)	0.003 (3.9)	0.009 (3.5)	NDA	102

Table 26. Column separation data for the 2nd irradiated LEU sulfate solution. Radioisotope concentrations (µCi mL^{-1}) were calculated from gamma spectroscopy to end of column time, 14.9076, except for the uranium concentrations which were measured by UV-vis spectroscopy as mol L^{-1} and subsequently converted to µCi mL^{-1}. EOB for this irradiation was 9.9278. Numbers in parenthesis are % errors. *^{105}Rh has poor activity balance.

	Fxn 1	Fxn 2	Fxn 3	Fxn 4	Fxn 5	Fxn 6	Fxn 7	Fxn 8	Fxn 9	Fxn 10	Fxn 11	Fxn 12	Fxn 13	Fxn 14	Fxn 15	Irreversibly bound to TiO_2 (µCi)	Activity balance (%)
pH	0.92	1.15	0.52	0.22	0.39	2.07	2.77	2.65	11.7	12.6	12.9	12.9	12.9	12.9	12.9	NDA	NDA
Volume	4.93	126.8	4.97	4.95	10.1	10.1	7.48	7.55	4.94	4.86	4.93	4.91	4.92	4.95	4.85	NDA	NDA
Uranium	1.04	1.58	1.09	0.09	NDA	NDA	NDA	NDA	NDA	NDA	NDA	NDA	NDA	NDA	NDA	NDA	100
^{239}Np 278 keV	2.33 (2.1)	4.77 (0.6)	3.42 (1.3)	0.42 (6.9)	NDA	NDA	NDA	NDA	NDA	NDA	NDA	NDA	NDA	NDA	NDA	NDA	100
^{141}Ce 145 keV	0.58 (0.6)	0.84 (0.7)	0.68 (1.4)	0.08 (10)	NDA	NDA	NDA	NDA	NDA	NDA	NDA	NDA	NDA	NDA	NDA	NDA	99
^{143}Ce 239 keV	1.34 (0.6)	2.07 (0.6)	1.62 (2.1)	1.66 (8.1)	NDA	NDA	NDA	NDA	NDA	NDA	NDA	NDA	NDA	NDA	NDA	NDA	100
^{140}Ba 537 keV	0.83 (0.9)	1.75 (0.9)	1.66 (1.9)	NDA	NDA	NDA	NDA	NDA	NDA	NDA	NDA	NDA	NDA	NDA	NDA	NDA	100
^{105}Rh 319 keV	0.21 (2.1)	0.45 (2.0)	0.47 (5.1)	NDA	NDA	NDA	NDA	NDA	NDA	NDA	NDA	NDA	NDA	NDA	NDA	NDA	58
^{95}Zr 757 keV	NDA	NDA	2.02 (1.3)	2.34 (1.2)	0.38 (0.8)	NDA	NDA	NDA	NDA	NDA	NDA	NDA	NDA	NDA	NDA	19(1.2)	98
^{97}Zr 743 keV	NDA	NDA	3.28 (0.9)	3.77 (0.8)	0.61 (0.9)	NDA	NDA	NDA	NDA	NDA	NDA	NDA	NDA	NDA	NDA	31(1.7)	87*
^{103}Ru 497 keV	0.10 (1.4)	0.15 (1.7)	0.70 (1.3)	0.84 (1.2)	0.16 (0.9)	NDA	NDA	NDA	NDA	NDA	NDA	NDA	$2e^{-3}$ (10)	$2e^{-3}$ (12)	$2e^{-3}$ (6.0)	17(0.7)	99
^{132}Te 228 keV	NDA	NDA	NDA	NDA	0.92 (0.6)	$9e^{-3}$ (1.3)	$5e^{-3}$ (17)	$9e^{-3}$ (2.9)	NDA	NDA	NDA	NDA	NDA	NDA	NDA	75(1.7)	19
^{131}I 365 keV	0.08 (1.6)	0.13 (3.7)	0.27 (2.1)	0.20 (1.6)	0.06 (1.5)	0.03 (1.2)	0.88 (0.5)	0.80 (0.7)	2.97 (0.8)	2.62 (0.6)	2.10 (0.7)	0.61 (0.5)	0.28 (0.6)	0.16 (0.6)	0.07 (0.6)	3(3.6)	70
^{99}Mo 181 keV	NDA	NDA	NDA	NDA	NDA	NDA	NDA	0.10 (11)	23.4 (0.8)	28.9 (0.8)	18.9 (1.2)	0.40 (2.6)	0.18 (3.1)	0.02 (3.1)	0.08 (3.0)	NDA	97
^{99}Mo 740 keV	NDA	NDA	NDA	NDA	NDA	NDA	NDA	0.09 (7)	22.9 (1.2)	28.5 (1.3)	18.7 (1.5)	0.40 (3.6)	0.19 (4)	0.15 (3.8)	0.08 (3.7)	NDA	93

Table 27. Column separation data for the 3rd irradiated LEU sulfate solution. Radioisotope concentrations (µCi mL^{-1}) were calculated from gamma spectrometry to end of column time, 31.9167, except for uranium concentrations which were measured by UV-vis spectrometry as mol L^{-1} and subsequently converted to µCi mL^{-1}. EOB for this irradiation was 28.0694. Numbers in parenthesis are % errors. * ^{97}Zr poor activity balance likely due in part to large % error in the production value.

Titania column separation	1st Irradiation	2nd Irradiation	3rd Irradiation
Volume of LEU sulfate feed (mL)	129	128	136
Volume of NaOH strip required for > 94 % ^{99}Mo recovery (mL)	9.3	9.7	22.3
^{99}Mo activity balance (%)	97	102	95

Table 28. Summary of the most significant column separation results, in terms of ^{99}Mo recovery.

	1st irradiation	2nd irradiation	3rd irradiation
% ^{131}I in uranium	8	24	22
% ^{131}I in 1 mol L^{-1} H_2SO_4/water washes	3	10	4
% ^{131}I in base pH < 11.7	35	21	16
% ^{131}I in base pH > 11.7	49	41	55
% ^{131}I in TiO_2 sorbent	5	3	3

Table 29. ^{131}I distribution among the different column fractions.

	1st irradiation	2nd irradiation	3rd irradiation
% ^{103}Ru in uranium	30	66	43
% ^{103}Ru in 1 mol L^{-1} H_2SO_4/water washes	27	12	20
% ^{103}Ru in base	< 1	< 1	< 1
% ^{103}Ru in TiO_2 sorbent	43	22	37

Table 30. ^{103}Ru distribution among the different column fractions.

	1st Irradiation	2nd Irradiation	3rd Irradiation
IO_3^- (%)	58	59	48
I_2 (%)	8	7	16
I^- (%)	34	34	36
Activity Balance (%)	86	33	76

Table 31. Iodine species in the three irradiated LEU sulfate solutions pre-separation. Percent in each fraction was calculated by dividing each fraction by the sum of all fractions. Data corrected to 72 hours after EOB.

	Fraction 2	Fraction 7	Fraction 9
pH	1.15	2.77	11.7
IO_3^- (%)	25	5	0
I_2 (%)	60	67	13
I^- (%)	15	28	87
Activity Balance (%)	70	69	75

Table 32. Iodine species in fractions 2, 7 and 9 for the 3rd irradiated LEU sulfate solutions. Percent in each fraction was calculated by dividing each fraction by the sum of all fractions. Data corrected to 72 hours after zero time.

	Half Life	1nd Irradiation	2st Irradiation	3rd Irradiation
^{103}Ru (497 keV)	39.28 days	6(0.3)	16(0.3)	15(0.3)
^{105}Rh (319 keV)	35.36 hrs	308(15)	257(9)	271(5)
^{131}I (365 keV)	8.04 days	7(0.3)	13(0.3)	18(0.3)
^{140}Ba (537 keV)	12.74 days	136(2)	151(2)	210(2)
^{141}Ce (145 keV)	32.50 days	46(0.3)	62(0.5)	89(0.6)
^{143}Ce (293 keV)	33.0 hrs	1173(14)	1085(10)	1405(8)
^{147}Nd (91 keV)	10.98 days	59(0.7)	63(1)	134(1)
^{239}Np (278 keV)	2.355 days	1267(10)	1095(10)	1444(9)

Table 33. Isotopes (and their concentration (µCi)) in fractions 2 of the three irradiated LEU sulfate solutions. Data corrected to 72 hours after EOB. Column end time for 1st = 349.0208; 2nd = 14.9076; 3rd = 31.9167. Time between EOB and column end for 1st = 2.9; 2nd = 5.0; 3rd = 3.8 days. Days between 1st/2nd and 2nd/3rd irradiations were 29.8 and 5.15, respectively.